UNIVERSITY OF TURKU

Embigin Function and Regulation in Human and Murine Macrophages

Department of Life Technologies

Molecular Systems Biology

Master's Thesis

Sajad Rahmani

12.6.2026

Turku

In loving memory of my father, Hossein,

who inspired me to never stop asking questions.

Master's Thesis

Subject: Molecular Systems Biology

Author: Sajad Rahmani

Title: Embigin Function and Regulation in Human and Murine Macrophages

Supervisors: Ph.D., Johanna Jokinen, Ph.D., Elina Siljamäki, M.D., Ph.D., Jyrki Heino

Number of pages: 70 pages

Date: 12.6.2026

Abstract:

Macrophages are the innate immune cells of the body, functioning as part of the physiological defence mechanism, as well as a finely tuned tissue repair system. Macrophages are categorized into two major classes of pro-inflammatory "M1" and anti-inflammatory "M2" macrophages, with tumor-associated macrophages being part of this class, where the pro-inflammatory cells drive defence responses while the anti-inflammatory macrophages mediate tissue repair and wound healing. This study aims to study the expression profile and potential functional roles of embigin, a membrane glycoprotein that has been associated with cell adhesion as well as developmental roles, in different macrophage populations from both mouse and human origins. Although embigin has been studied in other tissue types, its functions in macrophages remain unclear. This study utilizes a multi-method approach to identify the expression patterns and suggest potential functions for embigin in macrophages by analyzing multiple samples at the three biochemical landscapes of transcript, protein, and metabolite. The findings suggest that embigin is differentially expressed in macrophage subtypes, where the M2-like macrophages upregulate embigin transcripts as well as the embigin protein, demonstrated by the M2a subtype exhibiting the highest amount of embigin protein among the other M2-like phenotypes. Notably, the M2a phenotype is known to be the extreme end of anti-inflammatory activity, which underlines the correlation between embigin expression and anti-inflammatory polarization. Embigin is known to associate with monocarboxylate transporters (MCTs) as an ancillary protein facilitating their trafficking and function. This study finds different MCTs to be differentially expressed as well, with MCT1, mainly a lactate importer, being upregulated in M2-like macrophages, whereas MCT4, a lactate exporter, is downregulated, which indicates a change in the metabolic state of macrophages to favor lactate uptake. SMOC1, a protein previously shown to modulate phagocytic activity in macrophages, is upregulated in embigin knockout mice. Together, these results contribute to the further understanding of the roles of embigin in macrophages and provide potential future trajectories for immunology research focusing on embigin.

Keywords: embigin, lactate, macrophages, monocarboxylate transporters, SMOC1

Abbreviations

Arg-1	Arginase 1
BSA	Bovine Serum Albumin
CCL	Chemokine (C-C motif) Ligand
Cryo-EM	Cryogenic Electron Microscopy
ECM	Extracellular Matrix
$Emb^{-/-}$	Embigin Knockout
FBS	Fetal Bovine Serum
IFN-γ	Interferon Gamma
Ig	Immunoglobulin
IL	Interleukin
LIF	Leukemia Inhibitory Factor
LPS	Lipopolysaccharide
MAPK	Mitogen-Activated Protein Kinase
MCT	Monocarboxylate Transporter
M-CSF	Macrophage Colony-Stimulating Factor
MHC	Major Histocompatibility Complex
MMP	Matrix Metalloproteinase
NF-κB	Nuclear Factor Kappa B
PBS	Phosphate-Buffered Saline
PM	Peritoneal Macrophages
PMA	Phorbol 12-Myristate 13-Acetate

PRRs	Pattern Recognition Receptors
RNA-seq	RNA Sequencing
RT	Room Temperature
scRNA-seq	Single-Cell RNA Sequencing
SD	Standard Deviation
SDS-PAGE	Sodium Dodecyl Sulfate–Polyacrylamide Gel Electrophoresis
SEM	Standard Error of Mean
SMOC1	SPARC-Related Modular Calcium Binding Protein 1
TAM	Tumor-Associated Macrophages
TGF-β	Transforming Growth Factor Beta
Th1	T Helper 1 Cells
Th2	T Helper 2 Cells
TLR	Toll-Like Receptor
TME	Tumor Microenvironment
TNF	Tumor Necrosis Factor
VEGF	Vascular Endothelial Growth Factor
WT	Wild Type

Table of Contents

1 Introduction

1.1 Macrophages

Macrophages are innate and versatile immune cells that can be found in virtually all mammalian tissues, and they regulate the state of homeostasis as well as host defence. Macrophages in the tissues originate early in development from embryonic yolk sac progenitors, which seed tissues and mature into self-renewing and long-lived resident macrophages. While some of the macrophage populations are maintained by these embryonic cells, others are replenished from bone marrow-derived monocytes in adulthood, especially during inflammation. For instance, brain microglia cells arise from embryonic progenitors, whereas macrophages in the gut or in tumors originate from blood circulating monocytes (Guan et al., 2025).

Tissue macrophages have a morphologically large structure with abundant cytoplasm and surface extensions, with their membranes being rich in a variety of receptors for pathogens and dead cells. Functionally, they phagocytose (engulf) microbes, apoptotic cells, and debris, using enzymes and reactive oxygen species to digest the cargo and eliminate immune threats (S. Chen et al., 2023). Additionally, macrophages present antigens on major histocompatibility complex (MHC) class II molecules in order to activate T lymphocytes and, as a result, link the innate and adaptive immunity responses (Guan et al., 2025). Macrophages also secrete a wide variety of cytokines: pro-inflammatory factors such as tumor necrosis factor (TNF) and interleukin (IL) 12 that help kill the pathogens, while the anti-inflammatory factors (e.g., IL-10, TGF- β) help resolve inflammation and promote tissue repair (Ross et al., 2021).

1.1.1 Physiological properties of macrophages

The main function of macrophages is phagocytosis and clearance of debris. They express a variety of pattern-recognition receptors (PRRs), including C-type lectins and toll-like receptors (TLRs), to detect pathogens or damaged cells. After binding targets, macrophages engulf and internalize the target into phagosomes, which later fuse with lysosomes for degradation (Guan et al., 2025). Macrophages also continuously survey tissues and help maintain homeostasis by either secreting anti-inflammatory cytokines

or expressing phagocytic factors. For example, intestinal macrophages enter the gut lumen to sample microbes and help maintain gut homeostasis by the secretion of anti-inflammatory cytokines like IL-10. In the lungs, alveolar macrophages clear the inhaled particles while they express high levels of scavenger receptors for phagocytosis. During inflammation or infection, macrophages release cytokines, including TNF and IL-1β, to recruit other immune cells, like neutrophils, and induce fever (Guan et al., 2025).

Another key property of macrophages is antigen presentation. Macrophages degrade pathogens into peptides and load them onto MHC-II molecules within the endosomal/lysosomal compartments of macrophages intracellularly, and then localize them on the macrophage surface, thus presenting the antigens to T cells, resulting in their activation, which then initiates adaptive immune responses, linking innate and adaptive immunity (Guillaume et al., 2023). This antigen-presenting activity is coupled with co-stimulatory signals when macrophages are activated in a pro-inflammatory context. Additionally, macrophages secrete cytokines that shape the immune response landscape: classically activated macrophages mainly release IL-12 and interferon-gamma (IFN-γ) to promote T helper 1 (Th1) immunity, whereas the alternatively activated macrophages release IL-10 and TGF-β to support T helper 2 (Th2) responses and tissue repair (Guan et al., 2025; Strizova et al., 2023). Overall, macrophages serve as guardians and housekeeping cells, performing a range of physiological activities from detection of pathogens to resolution of inflammation, along with initiation of healing processes.

1.1.2 Macrophage subtypes and diversity

Macrophages may be activated in various ways, corresponding to different microenvironmental stimuli, contributing to their functional plasticity. This concept is often simplified into the classical M1 (pro-inflammatory) and alternative M2 (anti-inflammatory/wound healing) polarization states (Ma et al., 2022).

M1 macrophages are polarized by IFN-γ and lipopolysaccharide (LPS), and are strong effector cells that release pro-inflammatory cytokines such as TNF-α, IL-6, and IL-12, thereby promoting Th1 responses (Murray et al., 2014). On the other hand, M2 polarized macrophages driven by IL-4 and IL-13 cytokines demonstrate upregulated levels of arginase-1 (Arg-1), mannose receptor (CD206), and anti-inflammatory cytokines such as

IL-10, which functions in tissue remodelling, angiogenesis, and the overall resolution of inflammation (Martinez & Gordon, 2014).

The binary M1/M2 classification has therefore been challenged as an oversimplification failing to capture the full heterogeneity of macrophage populations. To address this, leaders in the field have proposed moving away from these limited labels in favor of a nomenclature that specifies the activation stimuli, such as M(IFN-γ), M(LPS), or M(IL-4), to more accurately reflect the distinct transcriptional and functional profiles induced by each inducing factor (Murray et al., 2014). This shift acknowledges that the M1 and M2 states are largely *in vitro* artifacts generated by defined, high-dose stimuli, whereas tissue resident macrophages *in vivo* encounter a diverse combination of signalling agents that generate a broad spectrum of functional phenotypes, rather than a simple bipolar switch (Mosser & Edwards, 2008).

The metabolic profile of different macrophage subtypes is intrinsically linked to their function; M1-like macrophages mainly rely on aerobic glycolysis, while the M2-like subtypes are associated with oxidative phosphorylation and fatty acid oxidation (O'Neill et al., 2016). A key metabolic interface in this process is the transport of lactate, a glycolytic end product, which is facilitated by monocarboxylate transporters (MCTs).

1.1.3 Tumor-associated macrophages (TAMs)

Macrophages are among the most abundantly recruited immune cell populations to the tumor microenvironment (TME), observed across all stages of tumor progression (Q. Zhang & Sioud, 2023). Collectively named tumor-associated macrophages (TAMs), they mainly arise from circulating monocytes, though tissue-resident macrophages also contribute to the TAM population (Q. Zhang & Sioud, 2023). When recruited to the TME by tumor-derived signals such as M-CSF, CCL-2, and CCL-5, TAMs are activated and then secrete growth factors, proteases, and immunosuppressive mediators that can help sustain tumor expansion, promote angiogenesis, and facilitate invasion and metastasis. Elevated levels of TAM are consistently associated with disease progression, therapy resistance, and poor survival across multiple solid tumor types, including lung, breast, hepatocellular, and gastric cancers (Goswami et al., 2021; Q. Zhang & Sioud, 2023).

TAM function is typically organized within the M1/M2 polarization landscape. Classical M1 polarization results in a pro-inflammatory tumoricidal phenotype, which is characterized by TNF, IL-12, and nitric oxide production. In contrast, the TME skews TAMs towards the anti-inflammatory M2 phenotype, which is pro-tumoral and associated with IL-10, TGF-β, and IL-6 secretion (Goswami et al., 2021; Q. Zhang & Sioud, 2023). This tumoral M2 phenotype bias is negatively correlated with survival across several cancer types. The extent of TAM heterogeneity has been further researched using single-cell multi-omics approaches, which have identified distinct populations of TAM subsets, such as interferon-primed, immune regulatory, lipid-associated, and proangiogenic populations (Ma et al., 2022).

Within the M2 spectrum, four functionally distinct subsets have been characterized more thoroughly: M2a, M2b, M2c, and M2d (Figure 1). Each subset is defined by its inducing stimuli, surface markers, and secretion outputs, yet all subsets share an IL-10^{high} and an IL-12^{low} cytokine profile (Q. Zhang & Sioud, 2023). The M2a subset is induced by IL-4 and IL-13 via STAT6 and PI3K/Akt signalling, and is characterized by high levels of CD206, CD209, and Arginase-1 expression; this subset drives tumor angiogenesis and invasion through CCL18 and vascular endothelial growth factor (VEGF) secretion. The M2b subset, also termed regulatory macrophages, requires co-stimulation by immune complexes and TLR agonists, like LPS, activating nuclear factor kappa-light-chain-enhancer of activated B cells (NFκB) and mitogen-activated protein kinase (MAPK) cascades. The M2b is characterized by its high CCL1 production, resulting in the recruitment of immunosuppressive Treg and Th2 cells, and expands with disease progression, as demonstrated in hepatocellular carcinoma (Q. Zhang & Sioud, 2023).

The M2c subset is induced by IL-10, TGF-β, or glucocorticoids, and signals through STAT3 to progressively suppress M1 activation. This subset is characterized by high CD163 and MerTK expression; a GAS6-MerTK positive feedback loop sustains IL-10 production, while VEGF and matrix metalloproteinase (MMP) secretion promote angiogenesis and matrix remodelling. Finally, the M2d macrophages, first identified in ovarian cancer ascites, are polarized by IL-6 and leukemia inhibitory factor (LIF) through JAK/STAT3 signalling; this subset is characterized by a $CD14^{high}$, $CD163^{high}$, TGF-β^{high} phenotype, and secretes VEGF and MMP9 along with the expression of immune checkpoint-related molecules, including

IDO, Siglec-15, and PD-1 ligands, and can thereby enable tumor immune evasion (Q. Zhang & Sioud, 2023). Overall, these M2 subsets facilitate tumor promotion and suppression of adaptive immunity, marking TAMs as a crucial contributor to an immunosuppressive TME.

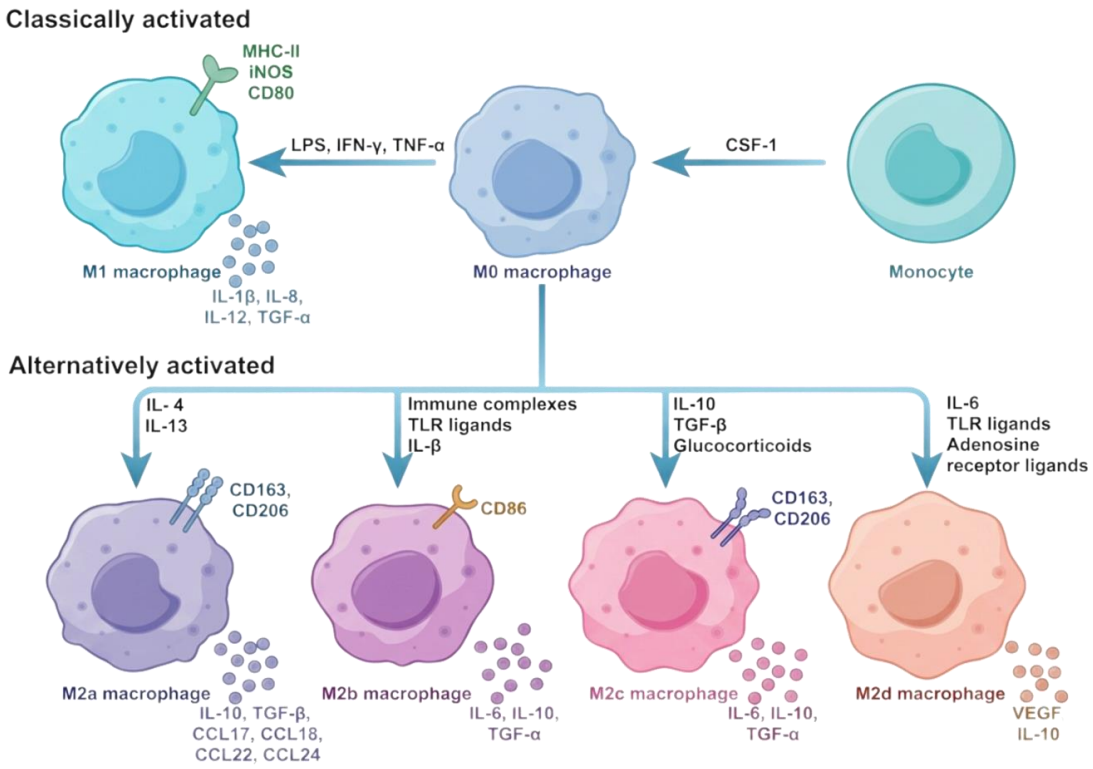

Figure 1. Monocytes can differentiate into naïve M0 macrophages, which can then be activated into the M1 or M2 macrophages. CSF-1 promotes the differentiation of monocytes into M0 macrophages. These cells can then polarize into M1 or M2 macrophages in response to Th1- or Th2-associated cytokines, respectively. Based on differences in activation state and function, M2 macrophages are further classified into four subtypes: M2a, M2b, M2c, and M2d. Different macrophage phenotypes express distinct molecular markers and secrete different mediators, thereby contributing to a range of physiological and pathological processes. CSF-1, colony-stimulating factor 1; MHC-II, major histocompatibility complex class II; iNOS, inducible nitric oxide synthase; LPS, lipopolysaccharide; IFN-γ, interferon-gamma; TNF-α, tumor necrosis factor-alpha; IL-1β, interleukin-1β; IL-8, interleukin-8; IL-12, interleukin-12. Figure adapted from Guan et al., 2025 using Biorender.

1.2 Monocarboxylate transporters (MCTs)

Monocarboxylate transporters (MCTs) belong to the solute carrier 16 (SLC16) gene family, made up of 14 members, of which only MCT1-4 have been confirmed as proton-coupled lactate transporters (Felmlee et al., 2020). These isoforms are integral membrane proteins with twelve transmembrane segments that facilitate the bidirectional, gradient-driven, co-transport of monocarboxylates and protons independent of ATP hydrolysis (Geistlinger et al., 2023). MCT1 and MCT4 require basigin (CD147), a surface glycoprotein for stable localization in the plasma membrane; its loss impairs the surface expression of these transporters (Afonso et al., 2015). Additionally, embigin (Gp70), another member of the basigin family, has also been shown to act as an ancillary protein, facilitating the trafficking of MCTs to the plasma membrane. Basigin has been demonstrated to mainly associate with MCT1, MCT3, and MCT4, whereas embigin is specifically associated with MCT2. Moreover, embigin has also been found to function as a facilitating ancillary protein for MCT1 when basigin is absent (Xu et al., 2022).

1.2.1 MCT-mediated lactate transport

Lactate, previously considered a metabolic waste, has recently been recognized as a central metabolite involved in intracellular energy transfer and cell signalling (Payen et al., 2020). MCT1-4 mediate the transmembrane movement of lactate by coupling monocarboxylate flux to the co-transport of protons along their electrochemical gradients, which makes the net transport direction entirely dependent on the combined concentration gradients of lactate and H^+ (Geistlinger et al., 2023).

In the intercellular lactate shuttle, glycolytic cells export lactate via MCT4, while oxidative cells nearby import it through MCT1 and utilize it for mitochondrial oxidation (Figure 2) (Xu et al., 2022). Transcriptional regulation of MCT expression is isoform-specific: MCT1 is induced by PPARα in oxidative tissues, while MCT4 is regulated by HIF-1α under hypoxic or high glycolytic conditions (Felmlee et al., 2020).

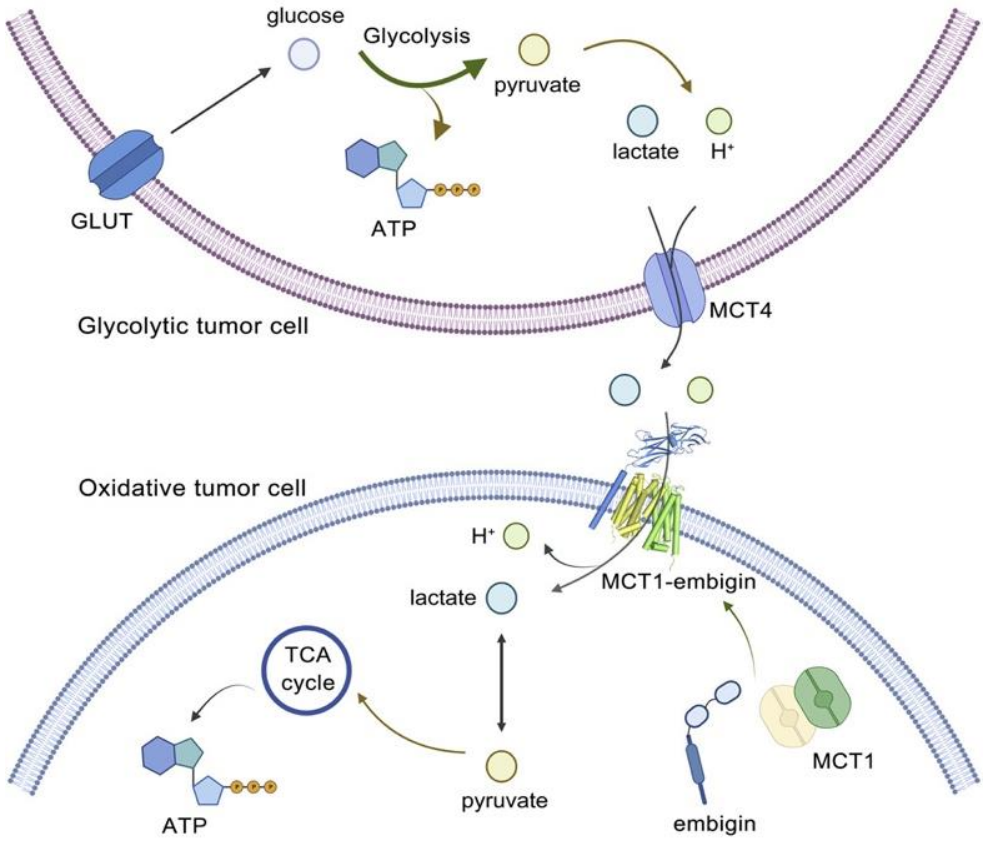

Figure 2. Lactate is transported between cells and the extracellular space via MCTs. Glycolytic cells drive glucose towards glycolysis, producing pyruvate, which is then turned into lactate and co-exported with H^+ outside the cell using MCT4. The oxidative cell can import the extracellular lactate using MCT1 and turn lactate into pyruvate, which is then driven towards oxidative phosphorylation. Embigin is found to associate with MCT1 and facilitate its localization into the plasma membrane. MCT: monocarboxylate transporter, GLUT: glucose transporter. Figure from Xu et al., 2022.

1.2.2 MCTs and cancer

Cancer cells mainly engage in aerobic glycolysis, known as the Warburg effect, generating excess amounts of lactate that must continuously be exported to sustain glycolytic flux and prevent intracellular lactate buildup and acidification (Afonso et al., 2015). This process makes tumor cells reliant on MCT1 and MCT4, both of which are broadly overexpressed in solid tumors and hematological malignancies compared to normal tissues (Payen et al., 2020). In the TME, a metabolic symbiosis is reached where glycolytic cancer cells export lactate via MCT4 and the oxidative tumor cells reimport it

through MCT1 as a respiratory substrate, a phenomenon named the reverse Warburg effect (Li et al., 2023; Pavlides et al., 2009).

Tumor-derived lactate accumulation in the TME helps drive cancer cell migration, angiogenesis, apoptosis resistance, and immune evasion (Jin et al., 2025). MCT4-dependent lactate secretion has been demonstrated to be a factor in antitumor immune suppression in a certain type of lung adenocarcinoma (Qian et al., 2023). Inhibition of MCT1 and/or MCT4 has been explored as a potential cancer treatment, resulting in intracellular lactate buildup, cell cycle arrest, and reduced tumor growth in multiple preclinical models; MCT1 inhibitors such as AZD3965 have even entered clinical trials (Koltai & Fliegel, 2024). Furthermore, high MCT1 and MCT4 expression has been demonstrated to be an independent prognostic factor across multiple cancer types, including breast, bladder, and renal cell carcinoma (Silva et al., 2023).

1.2.3 MCTs in macrophage subtypes

Macrophages exist on a functional spectrum of activation, ranging from pro-inflammatory M1-like macrophages, which have glycolytic metabolism and secrete cytokines such as IL-1β and TNF-α, and M2-like macrophages, which rely on oxidative phosphorylation and support tissue repair and tumor immune evasion (Tao et al., 2023). MCT1 and MCT4 expression are differentially regulated across the different macrophage polarization states: M1 polarization is associated with the upregulation of MCT4, while M2 polarization is correlated with an increase in MCT1 expression (L. Chen et al., 2025). MCT4 facilitates net lactate efflux from the cytoplasm in glycolytic M1-like macrophages, while MCT1 in M2-like macrophages is mainly localized in the mitochondrial membrane, directing intracellular lactate flux towards the citric acid cycle (TCA cycle), therefore, sustaining oxidative metabolism (L. Chen et al., 2025).

In the TME, TAMs are driven towards an immunosuppressive M2-like phenotype partly through MCT1-mediated uptake of tumor-derived lactate. Lactate influx into TAMs drives histone H3 lysine 18 lactylation (H3K18la) at the gene promoters of M2-associated factors, such as Arg-1, IL10, and VEGF-A, resulting in a pro-tumorigenic phenotype (Jin et al., 2025; Y. Zhang et al., 2024). It has been demonstrated that the inhibition of MCT4 in macrophages leads to the redirection of lactate towards H3K18la-mediated gene

activation cascades, supporting inflammation in atherosclerosis models (Y. Zhang et al., 2024). This underlines the broad immunomodulatory potential of targeting MCT-mediated lactate transport in disease contexts.

1.3 Embigin

Embigin (Gp70) is a highly glycosylated type I transmembrane protein (Figure 2) from the basigin subgroup of the immunoglobulin (Ig) superfamily. Together with basigin (CD147) and neuroplastin, embigin is a structurally conserved single-pass membrane glycoprotein, having two extracellular Ig-like domains, a hydrophobic transmembrane segment, and a short intracellular C-terminal tail (Figure 3). Embigin was first identified as a cell-surface molecule mainly expressed during early mouse embryogenesis, where it promotes integrin-associated cell adhesion (Huang et al., 1993; Ozawa et al., 1988). The human *EMB* gene is located on chromosome 5q11.1 and is translated into a core protein of ~37 kDa, which is heavily modified by N-linked glycosylation, resulting in a molecular weight range of 62 to 90 kDa (Guenette et al., 1997). The shared ability of all three members of the basigin subgroup to associate with monocarboxylate transporters and regulate their surface trafficking and localization underlines a common functional theme within this subgroup.

More recently, embigin has been characterized as a fibronectin receptor, directly binding to the N-terminal domain of fibronectin independently of canonical integrin interactions (Sipilä et al., 2022). Embigin knockout mice models have been used to study the stem cells (Silberstein et al., 2016). In addition, genetic knockout of embigin in mice results in delayed lung development and a neonatal mortality rate of 72%, which suggests a crucial physiological role for embigin during embryogenesis as well as functioning as a regulator in the early embryonic development of the kidney in mice. (Talvi et al., 2024, 2026).

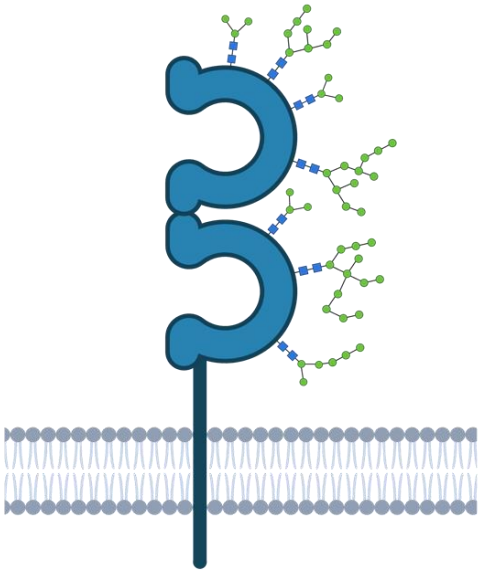

Figure 3. Glycosylated embigin is localized in the plasma membrane of cells. Embigin has two extracellular Ig-like domains and is highly glycosylated. The blue and green additions to the extracellular domains represent glycosylations. Illustration was made with Biorender.

1.3.1 Basigin family proteins

The basigin subgroup of the Ig superfamily consists of three members, basigin (CD147), embigin (Gp70), and neuroplastin (Np55/Np65), each functioning as a cell-surface chaperone, adhesion molecule, and metabolic regulator (Miyauchi et al., 1991). Basigin remains the most comprehensively studied member of the subgroup; it is broadly expressed across tissues and is well-known for its roles in the induction of MMP expression during tumor invasion, regulating retinal function, facilitating spermatogenesis, and, notably, acting as the primary ancillary protein for MCT1, MCT3, and MCT4 (Afonso et al., 2015). Neuroplastin, firstly identified as a synaptic adhesion molecule in the central nervous system, has been demonstrated to act as an ancillary protein for MCT2 by facilitating its localization to the neuronal plasma membrane (Beesley et al., 2014); additionally, it functions as an auxiliary subunit of plasma membrane Ca^{2+}-ATPases (Schmidt et al., 2017). Embigin is the founding member of the basigin subgroup, yet it remains less characterized.

1.3.2 Embigin associations with MCTs

Initially, embigin was identified as the main ancillary protein for MCT2 through studies in *Xenopus laevis* oocytes, which demonstrated that plasma membrane expression and functional activity of MCT2 were significantly increased by co-expression of embigin but not basigin (Wilson et al., 2005). Later research confirmed that while basigin preferentially associates with MCT1, MCT3, and MCT4, embigin serves as the primary ancillary protein for MCT2 but can additionally associate with MCT1 and facilitate its membrane trafficking (Figure 2) in tissues where basigin is absent (Xu et al., 2022). Embigin has been shown to associate with MCT4 and MCT7 as well (Cheng et al., 2025; Higuchi et al., 2022).

The molecular basis of embigin-MCT interactions has also been clarified using cryo-EM structures of the human MCT1-embigin complex resolved by Xu et al. (2022). This structure demonstrates that embigin forms extensive contacts with the transmembrane helices of MCT1, sterically preventing MCT1 homodimerization, therefore, promoting a conformational change in the transmembrane helix 5 that switches the transporter between certain substrate binding states (Xu et al., 2022). Cryo-EM structures from the analysis of the MCT2-embigin complex similarly demonstrate extensive transmembrane interactions that facilitate MCT2 membrane localization and modulate inhibitor sensitivity (Xu et al., 2025). These structural studies indicate that embigin not only acts as an ancillary protein for MCTs but also serves as an allosteric modulator that regulates transporter conformational states.

1.3.3 Embigin in macrophages

Although embigin has been described as an ancillary protein for MCTs and an embryonic regulator in mice, its expression and functional role in macrophages remain understudied. Single-cell RNA sequencing datasets and transcriptomic profiling studies have found embigin transcripts in myeloid cell populations, including monocyte-derived and tissue-resident macrophages, suggesting that embigin expression is not restricted to cells of the epithelial and stromal origin, but extends to innate immune cells (Sipilä et al., 2022; Talvi et al., 2024).

Given that macrophage polarization is linked to their metabolic regulation, with M1-like macrophages relying mostly on glycolysis and M2-like macrophages on oxidative phosphorylation, in addition to MCT-mediated lactate transport being an important factor in determining macrophage phenotypes (L. Chen et al., 2025), embigin may play a regulatory role in macrophage metabolism by modulating the availability and activity of MCT2 or MCT1 in a manner dependent on macrophage polarization states. To address these relatively incompletely characterized processes, this study aims to investigate the potential roles of embigin in a range of different macrophage subtype populations, both in human samples and mice.

1.4 SMOC1

Secreted protein acidic and rich in cysteine (SPARC)-related modular calcium binding 1 (SMOC1) is a secreted basement membrane glycoprotein found in several tissue types (Wang et al., 2022). Encoded by the *SMOC1* gene on chromosome 14q24.2, it contains five domains: an N-terminal follistatin-like domain, two thyroglobulin type-1 (Tg1) domains, a unique SMOC-specific domain, and an extracellular calcium-binding (EC) domain located at the C-terminal (Wang et al., 2022). In adult mice, SMOC1 expression has been detected in the liver and brain, and is reportedly expressed more during embryogenesis when the processes for the development of the eyes, limb buds, craniofacial structures, and somites are ongoing (Okada et al., 2011; Rainger et al., 2011).

Moreover, in mice, SMOC1 has been characterized as a direct transcriptional target of Runx2, which is the main osteoblast transcription factor, and its knockdown demonstrates the suppression of osteoblast differentiation and mineralization regulated by the Bmp2 signalling pathway (Takahata et al., 2021). In addition to skeletal development, SMOC1 has also been shown to modulate the BMP receptor II signalling and p38 phosphorylation, therefore regulating aortic valve calcification in a calcium-concentration-dependent manner (Wang et al., 2022). SMOC1 has also been identified as a platelet-derived thrombin activator, able to promote thrombin-induced platelet aggregation (Ukan et al., 2022). Overall, SMOC1 serves as a multifunctional glycoprotein

that regulates extracellular matrix (ECM) organization, along with growth factor signalling and coagulation pathways in developmental and disease contexts.

1.4.1 SMOC1 in macrophages

A study conducted by Ukan et al. (2022) investigated the effect of thrombin on macrophage polarization in murine bone-marrow-derived macrophages, providing direct evidence for a functional role of SMOC1 in macrophages. Thrombin stimulation polarizes an anti-inflammatory M2-like phenotype in macrophages, upregulating MRC-1, MMP9, and CD36, as well as secreting CCL22, inducing a TCA cycle metabolic profile that resembles the M2a macrophages, and enhances phagocytic activity against oxidized LDL and zymosan particles (Ukan et al., 2022). Interestingly, the addition of recombinant SMOC1 protein significantly increased thrombin-induced phagocytosis, while antibody-mediated blocking of SMOC1 or genetic haploinsufficiency ($SMOC1^{+/-}$) reduced the phagocytic activity, which was confirmed when recombinant SMOC1 was reintroduced, and the effects returned (Ukan et al., 2022).

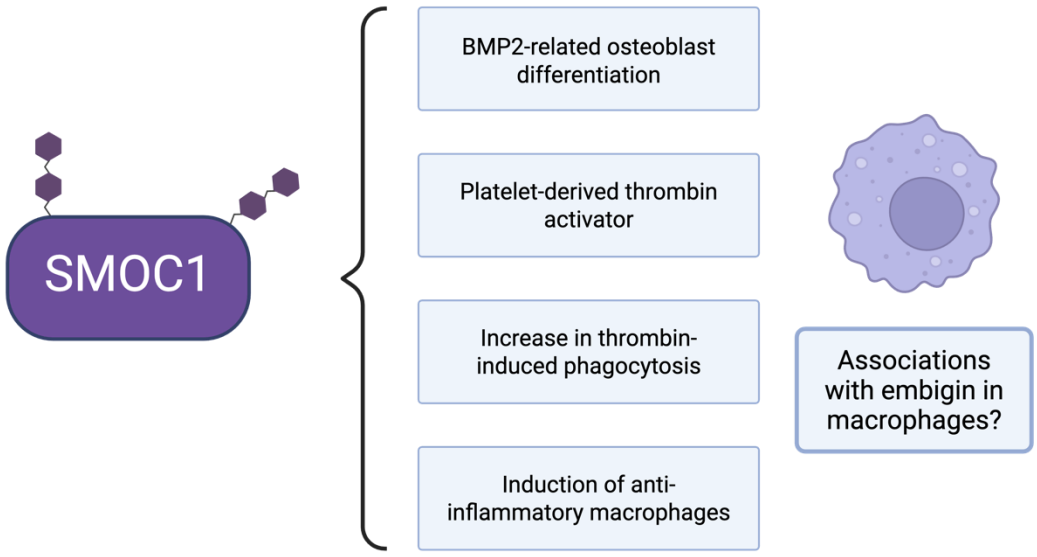

Figure 4. SMOC1 is a secreted glycoprotein with several known functions, but it is unclear if it has a link to embigin. SMOC1 is known to have a functional role in the BMP2-related osteoblast differentiation, platelet-derived thrombin activation, increased phagocytosis, and induction of anti-inflammatory macrophages. Illustration made with Biorender.

Additionally, at the transcript level, SMOC1 has an important impact on TGF-β-related genes in thrombin-stimulated macrophages. Antibody blocking of SMOC1 downregulated the thrombin-induced expression of some of the TGF-β and BMP signalling pathways, including Id1, Id3, Smad6, and Smad9, while increasing the expression of interferon-stimulated genes, resulting in a pro-inflammatory transcriptional profile in the macrophages (Ukan et al., 2022). These findings suggest that SMOC1 has a potential functional role in the regulation of thrombin-driven M2-like macrophage phenotype and phagocytic activity; however, whether SMOC1 is differentially expressed between M1- and M2-like polarization states or how SMOC1 regulates phagocytic activity and TGF-β signalling links to the immunosuppressive characteristics of TAMs, remains an open question for future research.

2 Aims of the Study

This study aims to investigate the expression profile and potential functional roles of the embigin protein in different macrophage populations with both human and murine origins. Previous studies have found embigin to be a fibronectin receptor, highlighting its role in modulating the interactions between cells and the ECM. Additionally, embigin has been shown to serve as an ancillary protein for the trafficking of certain MCT members, thus regulating cellular metabolism. Furthermore, recent studies have found embigin to have significant functions in the development of the lung and kidney in mice, as well as roles in stem cell regulation. With embigin being detected in macrophages, the results of this study were expected to unravel the expression profiles and suggest functions for embigin in macrophages. Accordingly, the aims of this study were to:

1. Characterize the transcriptomic profile of peritoneal macrophages in wild-type and embigin knockout mice by RNA sequencing.
2. Identify the expression profile of embigin at the transcript level in THP-1-derived human M1-like and M2-like macrophages.
3. Determine the extent of embigin at the protein level in both human-derived M2-like subtypes and mouse samples.
4. Visualize the embigin protein and its association with MCT proteins in primary murine peritoneal macrophage cells.
5. Analyze and suggest potential roles for embigin at the metabolic level, particularly, lactate transport between cells and the ECM.

3 Materials and Methods

This study utilizes a combination of methods to investigate the expression of embigin at the transcript and protein levels, and to identify potential functions at the metabolite level in both human- and mouse-derived samples.

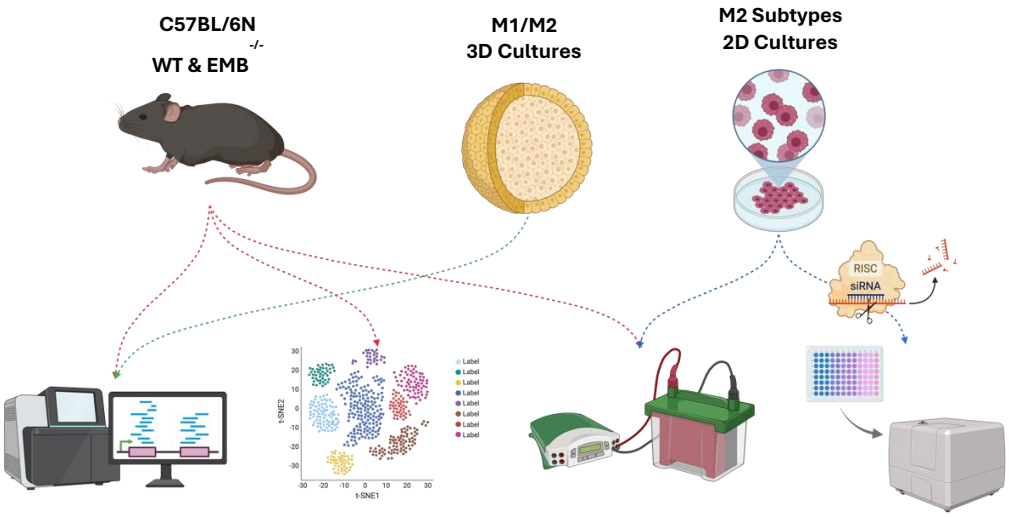

Figure 5. Overview of the materials and methods used in this study to investigate embigin expression and potential functions in different populations of macrophages across human and murine samples. This study utilizes a combination of methods to analyze multiple sample types at the transcript, protein, and metabolite levels. Both WT and Emb$^{-/-}$ phenotypes of C57BL/6N mice were used for RNA-seq and western blot analysis. A publicly available scRNA-seq dataset from murine peritoneal macrophages was analyzed using the Seurat software. Human M1- and M2- like spheroids were used for RNA-seq. 2D cell cultures of polarized M2 human macrophage subtypes derived from THP-1 monocytes were used for Western blot. A separate sample set of M2a cells was used to create embigin knockdowns using siRNA silencing and later used for fluorescence-based lactate assay. Illustration made with Biorender.

3.1 Animal Models

The wild type (WT) and embigin knockout (Emb$^{-/-}$) C57BL/6N mice (*Mus musculus*, Charles River Laboratories, Wilmington, MA) were maintained at the Central Animal Laboratory at the University of Turku (UTUCAL), Finland. The Emb$^{-/-}$ mice were engineered as previously described (Talvi et al., 2024). Genotype determination of the mice was performed by the Turku Center for Disease Modelling (TCDM). Mice aged between 8-10 weeks were selected for analysis.

All animal experiments were conducted under valid approval from the Ethical Committee for Animal Experimentation in Finland.

3.2 Cell Cultures

3.2.1 THP-1 monocytes

Human monocytic THP-1 leukemia cells (ATCC, TIB-202), which originated from the peripheral blood of an acute monocytic leukemia (AML) patient, were cultured in Iscove's Modified Dulbecco's Medium (IMDM) media (Gibco, catalog number: 12440053) with L-glutamine and 25 mM HEPES, supplemented with 10% fetal bovine serum (FBS), 50 µM β-mercaptoethanol (Thermo Fisher Scientific), penicillin (100 U/mL), and streptomycin (100 µg/mL), and approximately 6 million cells were seeded at 37 °C and 5% CO_2.

3.2.2 M2-like macrophage subtype polarizations

To polarize the different macrophage subtypes, 6 to 6.5 million THP-1 cells were cultured onto a Ø10 cm tissue culture dish and induced to an M0 macrophage state using 5 ng/mL of phorbol-12-myristate-13-acetate (PMA) (Sigma-Aldrich) for 3 days. After that, PMA was removed by changing the culture media back to the supplemented IMDM, and the cells were incubated PMA-free for 5 days. Then, the M0 macrophage cells were used to polarize the M2, M2a, M2c, and M2d phenotypes using a polarization medium consisting of 10 mL of the supplemented IMDM, with the corresponding polarization ILs, as listed in Table 2, and incubated at 37 °C and 5% CO_2 for 48 hours.

Table 1. Polarizing reagents used for M2-like subtype polarization

M2-like Subtype	Polarizing Agents and Concentrations
M2	IL-4 (20 ng/mL) + dexamethasone (100 nM)
M2a	IL-4 (20 ng/mL) + IL-13 (20 ng/mL)
M2c	IL-10 (50 ng/mL)
M2d	IL-6 (50 ng/mL)

3.2.3 3D macrophage spheroids

For RNA sequencing analysis of human THP-1-derived macrophages, the 3D spheroid cultures of M1- and M2-like macrophages were performed based on MISpheroID guidelines within an earlier study by Suwal et al. (2025), where the THP-1 cells were first differentiated into a monolayer of M0 macrophages by 5 ng/mL of PMA and then polarized

to M1-like macrophage spheroids by lipopolysaccharide (LPS) (10 pg/mL; Invitrogen) and interferon-gamma (IFN-γ) (20 ng/mL; PeproTech) induction for 24 hours, and M2-like macrophage spheroids by IL-4 (20 ng/mL; PeproTech) and dexamethasone (100 nM; Hellobio) polarization for 48 hours. (Suwal, 2025). The RNA sequencing samples used in this study were taken from the macrophage spheroids after the day 1 time point.

3.3 Murine Peritoneal Macrophage Isolation

Isolation of primary mouse peritoneal macrophages (PM) from 8–12-week-old WT and $Emb^{-/-}$ was carried out using an optimized version of the protocol developed by De Jesus et al. (2022). All animal procedures were performed in accordance with the approved IACUC euthanasia protocol. A 10 mL syringe was loaded with 5 mL of cold (stored at 4 °C) PM isolation media, 3% FBS in phosphate-buffered saline (PBS), and fitted with a 27-gauge needle and placed on ice immediately before each isolation (De Jesus et al., 2022). Immediately after euthanasia, the mouse was placed on a sterile surgical surface, and the limbs were secured. Then, the overlying skin was carefully incised and retracted to expose the intact peritoneal wall, as described by De Jesus et al. (2022). The peritoneal cavity was injected with 5 mL of PM isolation media; for smaller animals, the injected volume was reduced to prevent rupture of the peritoneal wall. The abdominal walls were then massaged gently in all directions to dislodge the adherent peritoneal cells into the suspension.

The lavage fluid was then recovered using a new 10 mL syringe fitted with a 25-gauge needle. As much fluid as possible was aspirated directly (typically the first ~4 mL), after which the peritoneal wall was incised, and any residual fluid was collected with a 1 mL Pasteur pipette. All recovered fluid was gently transferred into a 50 mL conical tube on ice, with the needle being removed from the syringe before emptying in order to minimize physical force on the cells.

Additional PM isolation media was added to each tube, bringing the total volume of the cell suspension to 30 mL, and cell culture was carried out according to the original protocol (De Jesus et al., 2022). The cells were incubated for 30 minutes at 37 °C with 5%

CO_2 to isolate the adhered macrophages from the other peritoneal cell populations, including B and T lymphocytes and epithelial cells. This time point was optimally minimized to allow for macrophage isolation in a manner that does not change the transcriptomic profile of the primary cells significantly over time. Following the incubation, the cells were washed with PBS to remove any non-adherent or dead cells. The remaining adherent cells were highly enriched in peritoneal macrophages and were then processed for RNA and protein extraction.

3.3.1 Primary cell preparations for immunofluorescence staining

Primary macrophages from the peritoneal cavity of mice were seeded on sterile glass coverslips (Ø12 mm), which were placed in (Ø3 cm) 6-well culture plates (four coverslips per plate) in 2 mL of RPMI 1640 (EuroClone) supplemented with 2 mM L-glutamine, 10% FBS, penicillin (100 U/mL), and streptomycin (100 µg/mL) and incubated at 37 °C and 5% CO_2 for two hours to allow for cell adhesion. The adhered cells were then used for immunofluorescence staining experiments.

3.4 Transcript-level Analysis

3.4.1 RNA isolation

Total RNA was extracted from 16 mouse peritoneal macrophage samples (4 male WT, 4 female WT, 4 male $Emb^{-/-}$, 4 female $Emb^{-/-}$) using the NucleoSpin TriPrep Kit (Macherey-Nagel) exactly following the manufacturer's instructions. The DNA was discarded, and the extracted RNA from the lysate was collected.

3.4.2 RNA concentration determination

RNA purity and concentration were determined using a spectrophotometric method (NanoDrop One, Thermo Fisher Scientific) by measuring absorbance at 260 and 280 nm with an acceptable threshold of A_{260}/A_{280} ratio of ≥2. The RNA samples were stored at -80 °C.

3.4.3 RNA sequencing

Bulk RNA sequencing of the mouse peritoneal macrophages was performed by the Finnish Functional Genomics Center (FFGC) at Turku Bioscience, Turku, Finland. Samples were submitted with a total RNA content of 1 µg, and the sequencing libraries were prepared accordingly. The Illumina NovaSeq X platform was used for paired-end sequencing of the samples. Raw data were returned as compressed FASTQ format for downstream analysis. The RNA sequencing analysis was mainly performed on Chipster (CSC Finland) (Kallio et al., 2011), a web-based bioinformatics tool used for quality control, reference genome alignment, read quantification, and differential expression analysis using tools such as MultiQC (Ewels et al., 2016) for quality control of the raw data, STAR paired-end read alignment tool (Dobin et al., 2013) to align the reads to the reference genome, HTSeq (Anders et al., 2015) for counting the aligned reads, and DESeq2 (Love et al., 2014) for differential expression analysis.

3.4.4 Single-cell RNA sequencing

To perform single-cell RNA sequencing analysis, a public query on the datasets available on Gene Expression Omnibus (GEO) was performed, and the dataset GSE210795 acquired from mouse peritoneal cells was selected for analysis. The single-cell sequencing analysis was mostly performed using the Seurat V5 (Hao et al., 2024) R package within the Chipster environment.

3.5 Protein-level Analysis

3.5.1 Protein isolation

To isolate the total protein content of the mouse peritoneal macrophage samples, after the RNA isolation, the flow-through of the NucleoSpin TriPrep Kit (Macherey-Nagel) was collected exactly following the manufacturer's instructions.

Protein isolation of the human-derived samples was performed using the typical RIPA protocol, where the cells were first washed once with ice-cold PBS and lysed directly on the tissue culture dish using cold (4 °C) Pierce RIPA buffer (Thermo Fisher Scientific) for 5

minutes on ice with occasional agitation. Then, the cell lysate was scraped using a cell scraper and transferred into a pre-chilled microcentrifuge tube and centrifuged at 14,000 g for 15 minutes at 4 °C. The supernatant, containing the protein sample, was recovered and stored at -20 °C.

3.5.2 Protein concentration determination

The total protein concentration of the mouse peritoneal macrophage samples was determined using the Pierce 660 nm Protein Assay (Thermo Fisher Scientific) according to the manufacturer's instructions. Bovine serum albumin (BSA) was used to create a protein standard curve.

A dilution series of BSA standards was prepared in PBS buffer in the following concentrations: 50, 100, 200, 500, 750, 1000, 1500, 2000 µg/mL. Protein samples were mixed with an equal volume of PBS (5 µL of sample + 5 µL of PBS).

To perform the assay, 10 µL of each standard or sample was pipetted into individual wells of a 96-well plate. Then, 150 µL of Pierce 660 nm Protein Assay Reagent was added to each well and mixed gently by pipetting. The plate was incubated at room temperature for 5 minutes. After that, the absorbance was measured at 660 nm using the Multiskan Go (Thermo Fisher Scientific) microplate reader. The blanks, one containing PBS only and one containing Pierce 660 nm Protein Assay Reagent only, were used alongside the standard curve to calculate and determine the final protein concentration of the samples.

3.5.3 Western blotting

To visualize and quantify sample proteins, Sodium Dodecyl Sulfate–Polyacrylamide Gel Electrophoresis (SDS-PAGE) was performed, and 8% polyacrylamide gels were used to run the samples. The running buffer was prepared using 25 mM Tris-base, 192 mM glycine, and 0.1% (w/v) SDS. To perform the transfer of proteins from the gel to the membrane, a transfer buffer consisting of 25 mM Tris-base, 192 mM glycine, and 20% (v/v) methanol was prepared and used. The transfer step was carried out in a cold room (4 °C) on ice.

The primary antibodies were used as listed in Table 3 and incubated on the membrane overnight. IRDye secondary antibodies (Table 3) were incubated on the membranes for one hour, and the Odyssey CLx (LI-COR Bioscience) imaging system, paired with the ImageStudio (LI-COR Bioscience) software were used to visualize the bands, followed by quantification by ImageJ/Fiji (Schindelin et al., 2012).

Table 2. Primary and secondary antibodies used in Western blot experiments

Antigen	Catalog #	Type	Company
Mouse Embigin	G7.43.1	Rat monoclonal	Invitrogen
Human Embigin	AB179801	Rabbit monoclonal	Abcam
SMOC1	AB313571	Rabbit monoclonal	Abcam
β-actin	A5441	Mouse monoclonal	Sigma-Aldrich
IRDye anti-rat IgG (800CW)	926-32219	Goat polyclonal	LI-COR Biosciences
IRDye anti-rabbit IgG (800CW)	926-32211	Goat polyclonal	LI-COR Biosciences
IRDye anti-mouse IgG (680CW)	926-68070	Goat polyclonal	LI-COR Biosciences

3.6 Immunostaining

3.6.1 Immunofluorescence staining of murine peritoneal macrophages

The growth media of the primary murine peritoneal macrophages, which were adhered to glass coverslips, were then aspirated, and the cells were rinsed once using PBS. The cells were then fixed using 1 mL of 4% formaldehyde in PBS and incubated for 20 minutes at room temperature (RT), followed by another PBS rinse. To allow for the detection of intracellular targets, cell membranes were permeabilized with 0.2% Triton X-100 in PBS (1 mL per plate) for 5 minutes at RT, followed by a PBS rinse.

The coverslips were transferred individually to different wells of a 6-well plate containing 1 mL PBS per well. Primary antibodies against embigin and MCT1 (listed in Table 4) were diluted 1:200 in 3% BSA in PBS. Then, the PBS was carefully removed by aspiration, and 30 µL of the prepared primary antibody solution was applied to each coverslip, followed by one hour of incubation at RT. The coverslips were then washed three times with PBS (5 minutes per wash).

Table 3. Primary and secondary antibodies used for immunofluorescence staining experiments

Antigen	Catalog #	Type	Company
Mouse Embigin	G7.43.1	Rat monoclonal	Invitrogen
Mouse MCT1	AB1286-I	Chicken polyclonal	Sigma-Aldrich
Anti-rat IgG (Alexa Flour 555)	A-21434	Goat polyclonal	Invitrogen
Anti-chicken IgG (Alexa Flour 488)	A-11039	Goat polyclonal	Invitrogen

The secondary antibodies, as listed in Table 4, were diluted 1:200 in 3% BSA in PBS. PBS was aspirated. 30 µL of the secondary antibody solution was added per coverslip, followed by a 30-minute incubation at RT in the dark. The coverslips were then rinsed once with PBS. Next, the nuclei were stained with DAPI diluted 1:1000 in 3% BSA in PBS (30 µL per coverslip) for 5 minutes at RT in the dark, followed by three 5-minute PBS washes.

The coverslips were mounted cell-side down on a microscopy slide using 4 µL of MOWIOL (Calbiochem) supplemented with 25 mg/mL DABCO (Sigma-Aldrich) as an antifading agent. The prepared slides were stored at +4 °C and imaged using the objective with 63x magnification on the LSM880 AiryScan (Zeiss) confocal fluorescent microscope.

3.7 RNA Interference

3.7.1 siRNA silencing of embigin in human M2a cells

THP-1 monocytes were differentiated and polarized to the M2a subtype, since the M2a macrophages express the highest levels of the embigin protein. Around 6×10^6 cells were seeded on Ø10 cm plates and treated with PMA to induce adhesion and M0 macrophage differentiation, followed by M2a polarization as described in 2.2.2.

RNA interference gene silencing was performed using human embigin-targeting siRNAs Hs_EMB_5 (Emb5) and Hs_EMB_8 (Emb8) (FlexiTube siRNA premix, Qiagen) and a non-targeting AllStars (Qiagen) negative control siRNA, all at the optimized final concentration of 5 nM, using siLentFect lipid transduction reagent (Bio-Rad) according to the manufacturer's instructions. Equal amounts of siLentFect and siRNA solutions were

combined and mixed by gentle tapping and then incubated for one hour at RT to allow for transfection complex formation. The siRNA concentrations, transfection incubation times, and cell conditions were optimized for macrophages prior to the main experiments, leading to the downstream analysis of lactate.

In parallel, M2a macrophages were harvested by a PBS wash followed by a 10-minute incubation with 1 mL of 5 mM EDTA at RT to detach the cells. The detached cells from a Ø10 cm tissue culture dish were then collected into a 50 mL tube, diluted with PBS to a total volume of 5 mL, and centrifuged at 200 g for 10 minutes. The supernatant was discarded, and the cell pellet was resuspended in supplemented IMDM growth media (similar to 2.2.1). Then, 400,000 cells were diluted with the appropriate amount of IMDM and seeded into each well of a 6-well plate.

For transfection, 750 µL of supplemented IMDM was added to each well of the 6-well plate, followed by 500 µL of the cell suspension (with a final cell count of 400,000 cells per well) and 250 µL of the appropriate siRNA-siLentFect complex. The plate was then gently mixed by moving around to ensure uniform cell distribution and exposure to the transfection complexes. After 4 hours of incubation at 37 °C and 5% CO_2, once the cells had adhered, the transfection media were replaced with 1.5 mL of fresh supplemented IMDM to reduce cytotoxicity associated with the transfection components. The cells were incubated for a total of 72 hours after transfection, after which the cells were collected for downstream experiments and analysis.

3.8 Metabolite-level Analysis

3.8.1 L-lactate assay of human M2a cells

To assess the lactate uptake and metabolism of the human THP-1-derived M2a cells, both wild-type controls and siRNA-mediated embigin knockdowns, the culture media lactate concentration was measured using a fluorometric L-lactate assay kit (AB65330, Abcam) according to the manufacturer's instructions. After a 72-hour siRNA transfection, the culture medium was replaced with 2 mL of serum-free IMDM. Next, after 4 hours of incubation at 37 °C, 200 µL of the medium was collected from each of the samples

(AllStars control, Emb5, Emb8) and centrifuged at 200 g for 10 minutes at RT, and the supernatant was used for the assay. The cells were then detached and counted to allow for a normalization of lactate values to the cell number.

All reagents and standards were prepared according to the manufacturer's instructions. The media samples were diluted 1:750 in Assay Buffer 2. The dilution range of 1:500 – 1:1000 was determined to fall within the linear range of the standard curve for 4-hour lactate secretion from M2a macrophages.

The assay was performed in a black 96-well plate with clear bottoms. Standard and sample wells each received 50 µL of the respective standard dilution or the 1:750 diluted samples. Background control wells received 50 µL of the 1:750 diluted sample without the Enzyme Mix. The reaction mix was prepared according to the manufacturer's instructions, and 50 µL was added to the reaction wells. Background control wells received the same, but without the Enzyme Mix. Then, the mixtures were pipetted gently to ensure proper mixing and incubated at RT for 30 minutes while being protected from light exposure. Finally, fluorescence was measured at excitation/emission wavelengths of 535/587 nm by a Sense (Hindex) microplate reader.

Lactate concentrations were calculated by subtracting the blank (Assay Buffer 2 only) reading from all the values and subtracting the sample background control reading from the sample readings (in each experiment where the background reading was significant). The lactate amounts were then determined from the standard curve and converted into concentration values using the formula provided by the instructions. The final lactate concentrations were normalized to the cell numbers. The experiment was carried out for 7 total replicates, including technical replicates across 3 sets of biological replicates.

3.9 Statistical Analysis

All statistical analyses and visualizations were performed using R (R Core Team) and Chipster (CSC Finland). For comparisons across multiple sample groups, one-way analysis of variance (ANOVA) was employed, followed by Tukey's Honestly Significant Difference (HSD) test to identify pairwise differences while controlling for multiple comparisons. Where appropriate, pairwise comparison between two groups was performed using Welch's two-sample t-test, which does not assume equal variance between groups. Bulk RNA sequencing and single-cell RNA sequencing data were analysed by the built-in workflows and tools available in the web-based bioinformatics software Chipster. The results were considered statistically significant at the threshold of $p < 0.05$.

4 Results

To reach the aims of the study, both human-derived samples and murine samples were studied at different biological levels. Mouse experiments were designed to achieve full knockout of the embigin gene, thus yielding results with minimal residual expression of embigin. Furthermore, the peritoneal macrophages are known to have a mainly anti-inflammatory M2-like phenotype (Cassado et al., 2015), so $Emb^{-/-}$ mice are appropriate samples to characterize potential embigin functions in alternatively activated tissue-resident macrophages. Additionally, murine experiments allow for studying *in vivo* conditions where no external stimuli are applied, and the macrophage phenotype is as close to the physiological conditions as possible.

Although mouse experiments are highly valuable, it is quite important to validate the results of these experiments by performing similar experiments on human-derived samples. The results obtained from human-derived samples account for any possible species-specific variations between humans and mice. Additionally, these human-derived samples are more well-studied and are simpler to work with when paired with downstream experiments. Therefore, THP-1-derived macrophages are used in this study to generate embigin knockdown cells and analyze them through lactate assays to find potential links between embigin expression and lactate transport regulation.

Altogether, the results obtained from both human- and mouse-derived samples provide coherent evidence that embigin expression is linked to the phenotypic status of macrophages, as well as suggesting that the metabolic regulation changes with the presence of embigin.

4.1 Human M2 cells exhibit higher embigin expression at the transcript level

To investigate the expression profiles of embigin in the human-derived M1- and M2-like macrophage subtypes, RNA-seq data obtained from human spheroid models of both M1- and M2-like cells were analyzed. The results demonstrated that the transcriptomic profile of the M1-like and the M2-like macrophages is significantly different, and embigin was upregulated by 47% (Log2FC = 0.5543) in M2-like macrophage subtypes when compared with M1-like cells across a set of 4 biological replicates (Figure 6).

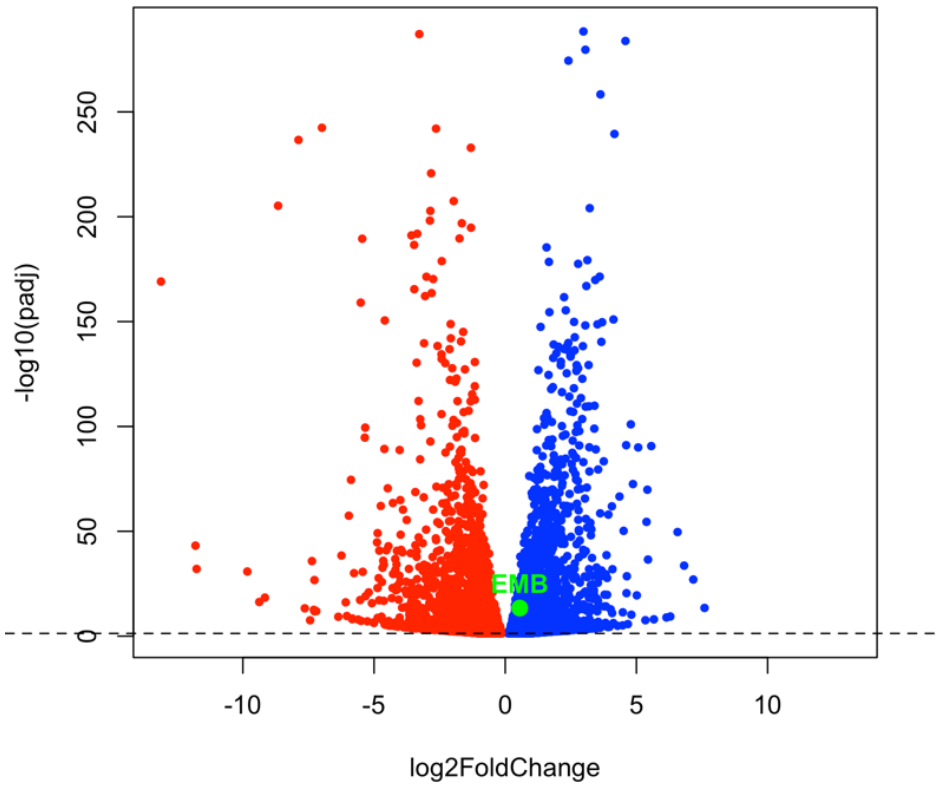

Figure 6. Embigin is upregulated in the M2-like macrophages compared to the M1-like macrophages. Volcano plot for human THP-1-derived M2-like macrophage spheroids, generated from bulk RNA sequencing data. Genes in blue are upregulated in M2-like macrophages compared with M1-like macrophages, and the genes in red are downregulated. Embigin is highlighted in green.

4.2 MCTs are differentially expressed in human macrophage subtypes

The RNA sequencing data from human M1-like and M2-like macrophages also reveal that several members of the monocarboxylate transporter family are differentially expressed. MCT1 (*SLC16A1*), which is known to have a high affinity for lactate, often acting as an importer to transport lactate inside the cell for oxidation, is significantly upregulated in M2-like cells at the transcript level, with 130% (Log2FC = 1.2029) higher reads compared with M1-like cells. MCT8 (*SLC16A2*) (Log2FC = 0.4238) and MCT6 (*SLC16A5*) (Log2FC = 0.4708) are slightly upregulated in M2-like cells (Figure 7, B).

On the other hand, MCT4 (*SLC16A3*), characterized as a lactate exporter, is found to be downregulated significantly in M2-like cells (Log2FC = -1.2899) compared with M1-like macrophages. Furthermore, MCT2 (*SLC16A7*) (Log2FC = -0.9134) and MCT10 (*SLC16A10*) (Log2FC = -0.9511) are downregulated in M2-like human macrophage subtypes in comparison with M1-like populations (Figure 7, B).

Based on the number of read counts assigned to each gene, MCT4 is the most expressed MCT in macrophages, along with MCT1, which has quite a high number of transcripts, comparable with embigin. In contrast, MCT8, MCT6, MCT2, and MCT10 demonstrate a lower number of total transcripts in both M1- and M2-like macrophages (Figure 7, A). This highlights that in the context of macrophages, MCT1 and MCT4 are the most relevant members of the monocarboxylate transporters. Since both are known to be strongly associated with lactate transport, it is noteworthy that embigin upregulation is correlated with MCT1 upregulation and MCT4 downregulation at the transcript level, which may result in certain distinct metabolic regulatory processes in pro- and anti-inflammatory macrophages.

A)

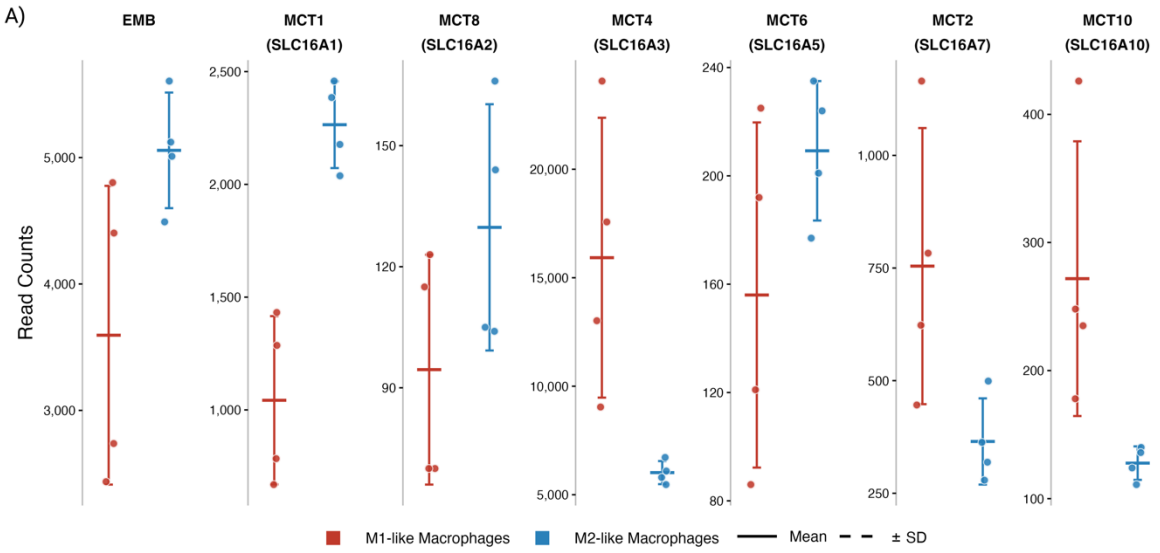

B)

Symbol	Protein	log2FoldChange	FoldChange (higher in M2)	padj
EMB	Embigin	0.5543	1.47	4.00E-14
SLC16A1	MCT1	1.2029	2.30	2.10E-89
SLC16A2	MCT8	0.4238	1.34	2.80E-02
SLC16A3	MCT4	-1.2899	-2.45	1.00E-54
SLC16A5	MCT6	0.4708	1.39	5.90E-04
SLC16A7	MCT2	-0.9134	-1.88	3.10E-10
SLC16A10	MCT10	-0.9511	-1.93	1.40E-08

C)

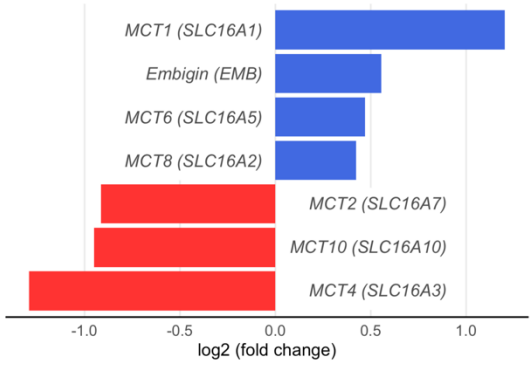

Figure 7. Embigin and MCT family genes are differentially expressed in M1- and M2-like human macrophage spheroids. A) Multifaceted scatter plot of the number of read counts of embigin and MCT family genes in M1- and M2-like macrophage spheroids. Mean ± 1 SD is shown. **B)** Calculated fold changes of embigin and the MCT family genes in human M1- and M2-like macrophages. Positive numbers denote a higher number of read counts in the M2-like macrophages, while negative values represent downregulations in the M2-like macrophages compared with M1-like samples. **C)** Differential expression bar plot for the M1- and M2-like macrophages. The genes in blue are upregulated in the M2-like macrophage spheroids, while the genes in red are downregulated in the M2-like macrophages when compared with M1-like macrophage spheroids.

4.3 Macrophages are diverse and complex at the single-cell resolution

With the aim of validating that embigin is also expressed in tissue-resident macrophages of the peritoneal cavity and analyzing the heterogeneity of macrophages at the single-cell resolution, the publicly available GEO dataset GSE210795 was used, which was acquired from mouse peritoneal cells. The data includes more than 13,000 cells within 22 clusters (Figure 8, A).

After visualization of embigin, the data suggests that only a fraction of the cells express embigin at a significant level. These *Emb*$^{+}$ cells could fall into one cluster, cluster 9 in this case, or be scattered within the other cell clusters as well (Figure 8, B).

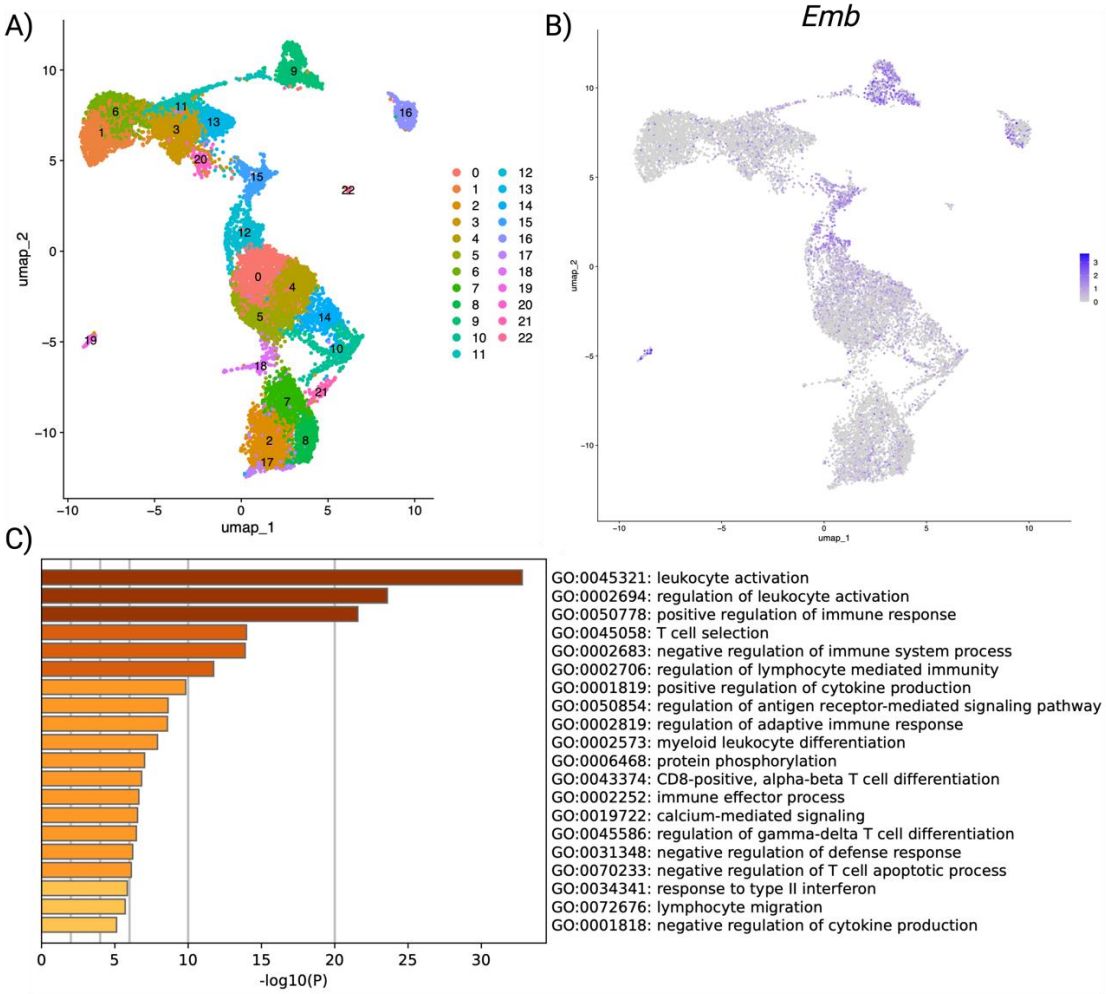

Figure 8. Mouse peritoneal macrophages are highly diverse, and embigin is significantly expressed in some clusters of cells. A) UMAP of scRNA-seq data clusters. The dataset was acquired from mouse peritoneal cells and was analyzed using Seurat v5. GEO dataset: GSE210795. **B)** Visualization of the *Emb* gene in the scRNA-seq data. Emb transcripts can be found in cells in different amounts. **C)** Gene enrichment analysis for the differentially expressed genes in cluster 9. The GO biological processes related to the differential expression of genes are demonstrated.

Enrichment analysis on the differentially expressed genes in cluster 9 suggests that regulatory processes for the immune system response pathways are being affected. Leukocyte activation and the positive regulation of the immune responses are among the most significantly differentially expressed biological pathways (Figure 8, C).

In addition to embigin, the genes for MCTs were also visualized on the UMAP, which demonstrates that different MCTs are also being expressed to different extents in different clusters of cells and underlines the level of heterogeneity in macrophages (Figure 9).

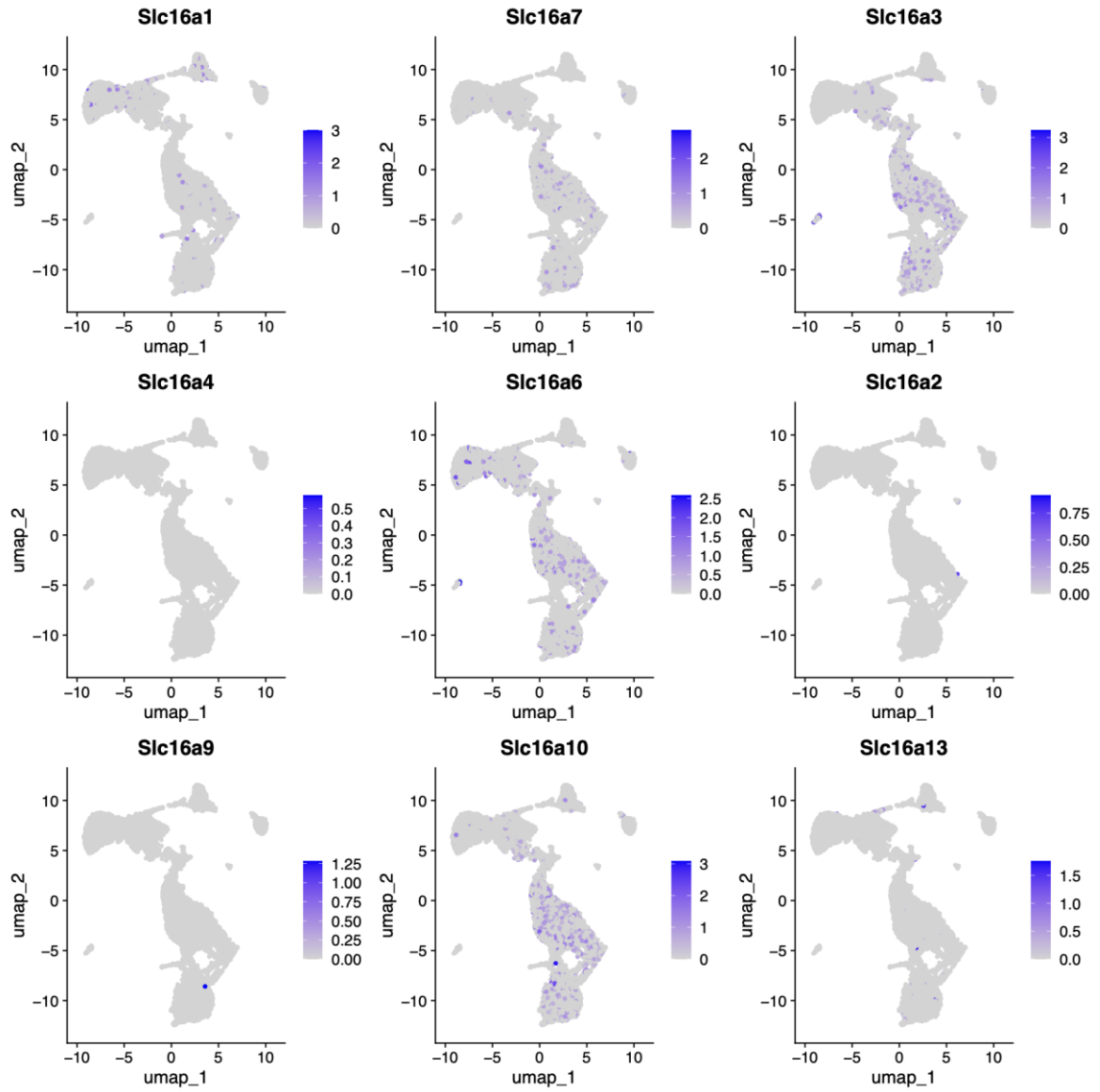

Figure 9. MCT members are differentially expressed in mouse peritoneal macrophages, underlining the heterogeneity of macrophage phenotypes. The plots show different relevant MCT members visualized on cell clusters. Slc16a1: MCT1, Slc16a7: MCT2, Slc16a3: MCT4, Slc16a4: MCT5, Slc16a6: MCT7, Slc16a2: MCT8, Slc16a9: MCT9, Slc16a10: MCT10, Slc16a13: MCT13.

Pairwise analysis of the most relevant MCT genes to embigin, namely MCT1, MCT2, and MCT4, shows that not all cells or clusters that are *Emb*$^{+}$ are necessarily positive for either of the MCTs, which introduces additional complexity in the phenotypic states of macrophages present in one population (Figure 10).

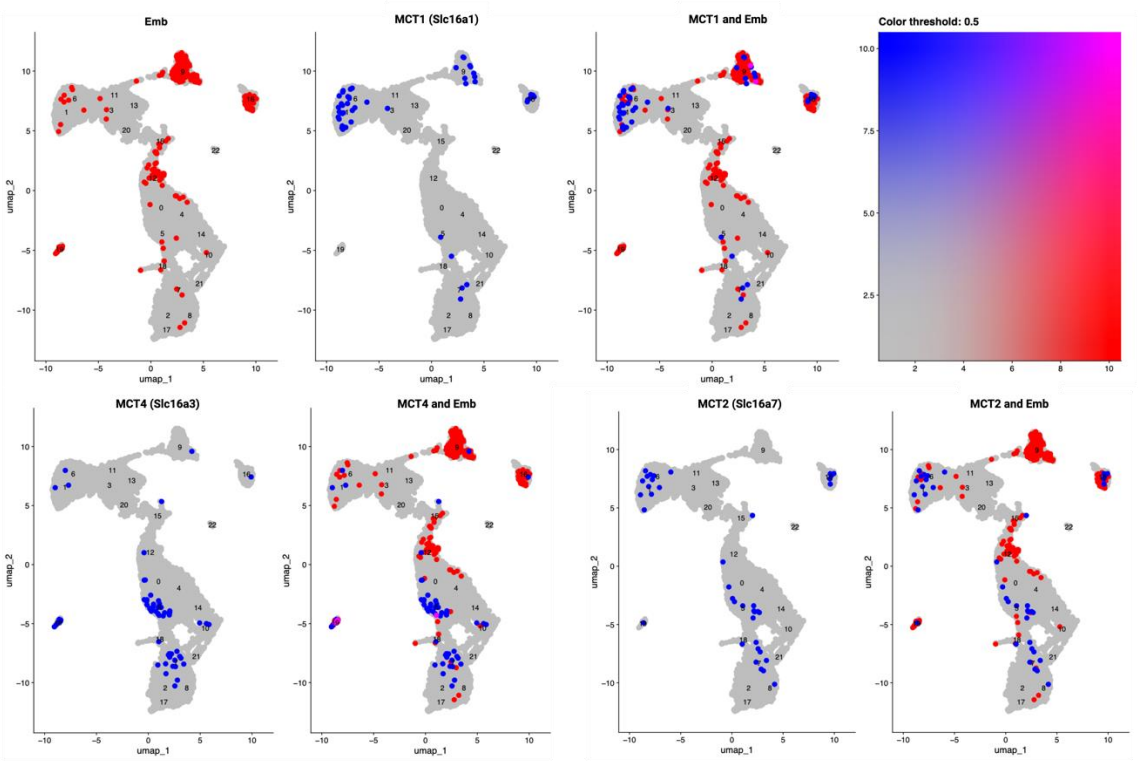

Figure 10. Embigin is significantly expressed along with MCT1, MCT2, and MCT4 in certain cells in certain macrophage population clusters. Pairwise visualization of the embigin transcripts, along with the different MCT genes associated with metabolism and lactate transport. When both genes are present at high levels, the color shifts towards purple. Slc16a1: MCT1, Slc16a7: MCT2, Slc16a3: MCT4

4.4 The human M2a subtype has higher expression of embigin at the protein level

For the purpose of validating that embigin is not only upregulated at the transcript level but is also increased at the protein level in the M2-like macrophages, Western blot experiments were performed on THP-1-derived human M2, M2a, M2c, and M2d macrophage subtypes. These experiments were also aimed at identifying which macrophages express the highest amount of embigin protein.

The results from 3 biological replicates consistently demonstrate that the M2a subtype has the highest expression of embigin at the protein level, compared with M2 (polarized with IL-4 and dexamethasone), M2c, and M2d macrophages. In addition, the M2d phenotype exhibits the lowest amount of embigin, while the M2 and M2c phenotypes approximately express embigin at similar levels (Figure 11).

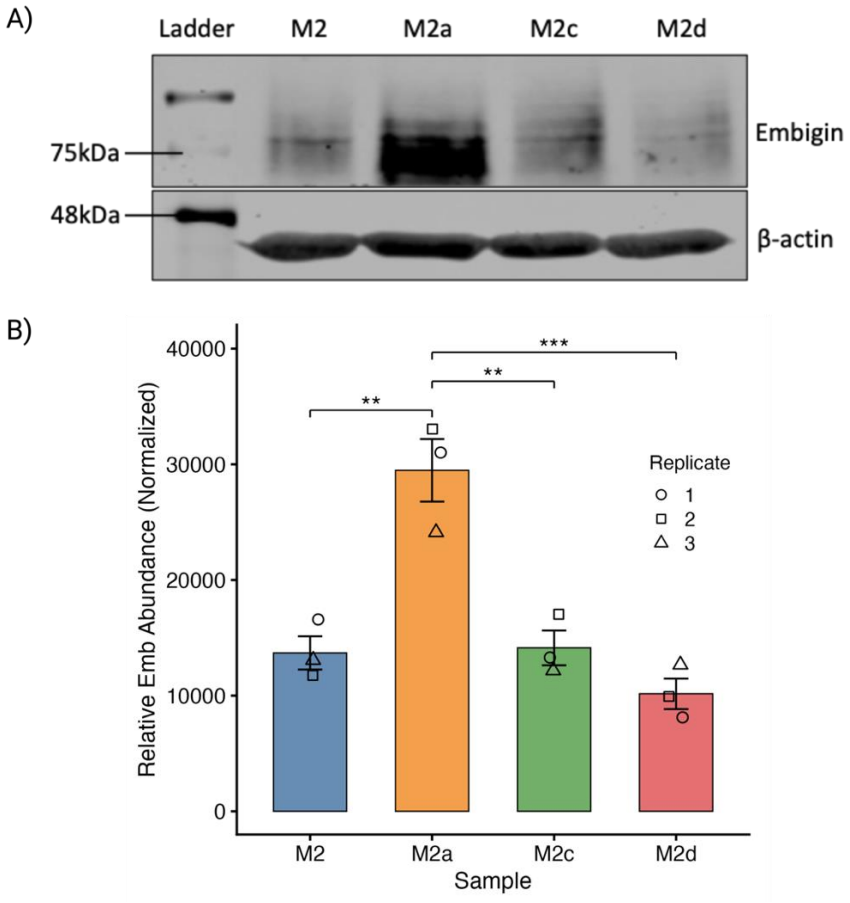

Figure 11. The human M2a macrophage expresses the highest amount of embigin protein. A) One of the biological replicates is represented in the Western blot of M2-like 2D cultured human macrophage subtypes. SDS-PAGE with an 8% gel was used to run the samples for western blotting. **B)** Quantified bar chart of the embigin expression in M2 macrophage subtypes. One-way ANOVA p-value = 0.0003. Biological replicates: 3, mean ± standard error of mean (SEM) is shown; **: $p \leq 0.01$, ***: $p \leq 0.001$

4.5 An optimized protocol for siRNA silencing of embigin in THP-1-derived macrophages

Since acquiring mouse samples for metabolic studies would be very challenging, this study focused on an alternative method for generating embigin knockdowns to somewhat mimic the $Emb^{-/-}$ conditions. RNA interference (RNAi) was selected to target the embigin transcripts and inhibit their translation into proteins; however, the protocol for reliably performing siRNA-mediated embigin inhibition was not optimized for macrophages in terms of siRNA concentration, transfection incubation times, and cell conditions, prior to this study.

In order to achieve an optimized and reliable method of knocking down the embigin transcript in the THP-1-derived M2a macrophages, different siRNA concentrations and incubation conditions were tested. At first, it was thought that transfecting the already adhered macrophages would be best since it would not require detaching and potentially damaging the cells in the process. Two different time points of 48 and 72 hours were also tested for both Emb5 and Emb8 siRNA transcripts to target the embigin mRNA, and the outcomes were assessed via western blotting. β-actin was used as a control measure of cell viability and a normalization base for quantifying the embigin protein levels, while the Allstar siRNA was used as a control measure for the toxicity of the transfection solution and the siRNAs. It was deduced that with the 50 nM siRNA concentrations, adherent transfection, both at the 48h and the 72h time points, was not practical at all when compared with in-solution transfection. In addition, it was found that the 48h time point was also very inconsistent in terms of knockdown efficacy, so the 72h incubation time was selected for further optimization (Figure 12).

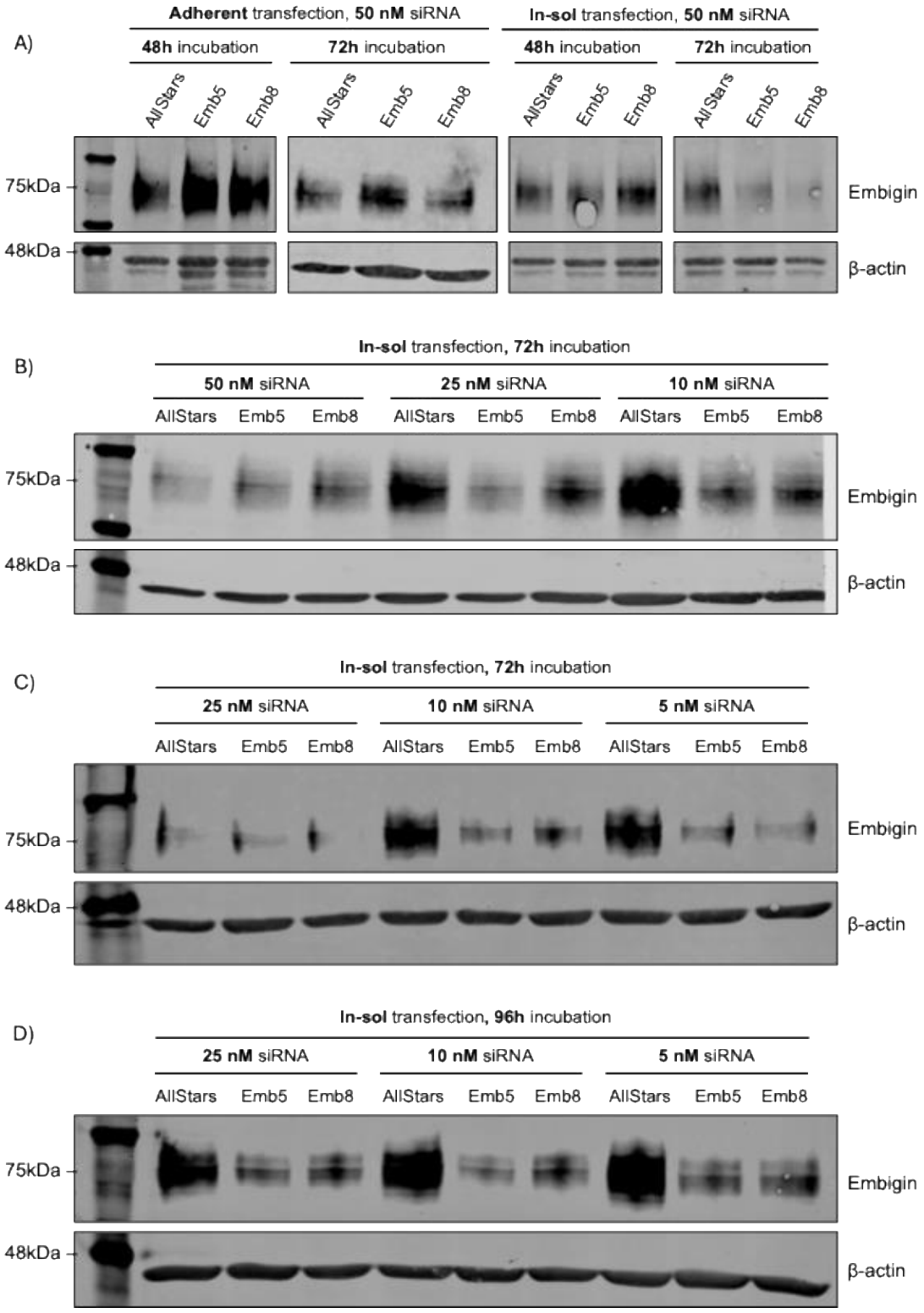

Figure 12. The optimized conditions for embigin knockdown in THP-1-derived M2a macrophages are in-solution transfection, using 5 nM siRNA, and incubated for 72 hours. A) Adherent and in-solution siRNA transfection of THP-1-derived M2a macrophages. The siRNA concentration was 50nM. **B)** In-solution transfection using different siRNA concentrations and a 72h incubation time. **C)** In-solution transfection using different siRNA concentrations with a focus on the new 5 nM concentration with 72h incubation. **D)** In-solution transfection using different siRNA concentrations with a focus on the new 5 nM concentration with 96h incubation. SDS-PAGE with an 8% gel was used to run the samples for western blotting. In-sol: in-solution.

To proceed further with the knockdown optimization of in-solution transfections, lower siRNA concentrations were also tested, as higher concentrations had negative effects on cell viability. It was observed that the lower siRNA concentrations are also functional in knocking down the embigin protein. Additionally, with the lower concentrations, a significantly smaller number of dead cells were observed after the 72h incubation step (Figure 12, B).

Finally, to test if the incubation time could be further increased, a test run with an incubation time of 96 hours was also performed. In this test, a lower concentration of 5nM siRNA was also implemented. The results showed that the 96h incubation time had a lower knockdown efficacy compared to the 72h, with a knockdown percentage of 70.6% for Emb8 after 96 hours compared to 78.5% for Emb8 after 72 hours. Furthermore, the 5 nM concentration was proven to be the best of both worlds: having the best embigin knockdown efficacy while being the least toxic to cell viability (Figure 12, C, D). Overall, these results lead to the optimized conditions for consistent embigin knockdown in M2a macrophages: in-solution transfection of 5 nM siRNA concentrations, followed by a 72h incubation time (Figure 13).

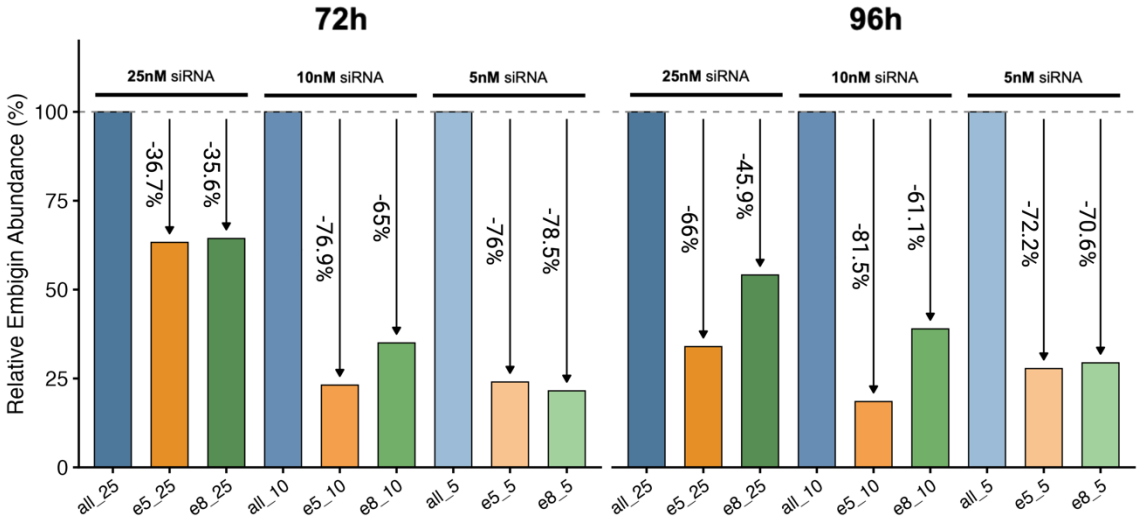

Figure 13. Optimization of the siRNA transfection conditions for the knockdown of embigin. In-solution siRNA transfection of THP-1-derived M2a macrophages with different siRNA concentrations after 72h and 96h incubations. SDS-PAGE with an 8% gel was used to run the samples for western blotting, and the bands were quantified. Relative embigin presence in the knockdown samples compared with the AllStars control. The arrows represent the knockdown percentage by quantifying the decrease in embigin protein in the samples.

4.6 There is no significant change in MCT-mediated lactate transport in human M2a embigin knockdowns

To investigate the metabolic relevance of embigin in macrophages, lactate assay experiments were designed using THP-1-derived M2a cells, since this subtype expresses embigin protein the highest among M2 subtypes. First, M2a WT cells and embigin knockdowns were generated through siRNA-mediated inhibition, and then the lactate secreted by the cells into the culture media was isolated and analyzed by a fluorescence-based lactate assay kit to measure the total lactate concentration in the extracellular environment with a total of 7 biological replicates.

Results yielded by the assay were not statistically significant with a P-value of 0.592. However, it is noteworthy to notice that the embigin knockdown samples have a higher lactate concentration of about double that of the control, in the culture media (Figure 14).

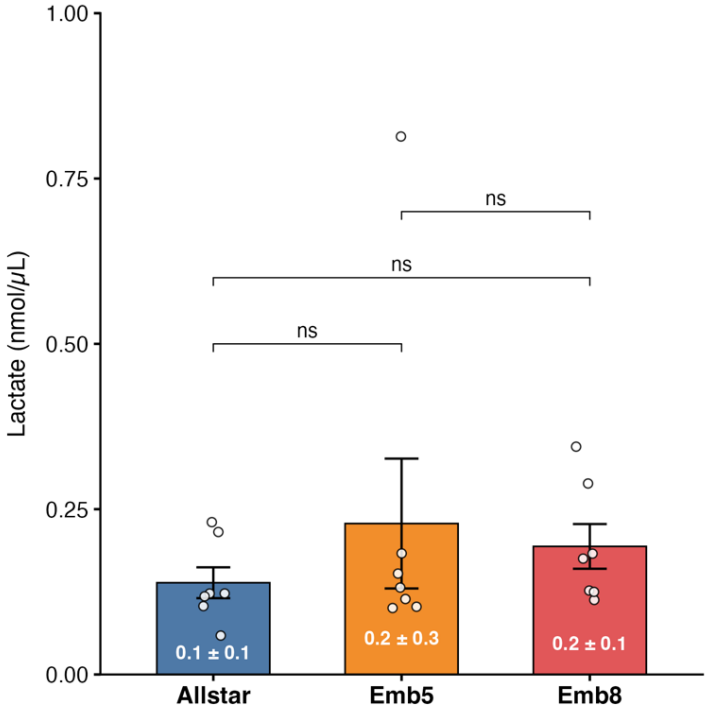

Figure 14. Culture media lactate concentration of the WT and embigin-knockdown human M2a macrophages. Mean ± SEM is shown. Allstar: AllStars WT control samples, Emb5: embigin-knockdowns using the Emb5 siRNA, Emb8: embigin-knockdowns using the Emb8 siRNA, biological replicates: 7.

4.7 Transcriptome characterization of murine peritoneal macrophages

To investigate the effects of embigin knockout *in vivo*, 16 samples of male and female WT and Emb$^{-/-}$ mouse models at the age range of 8-12 weeks old were selected, and macrophages localized in their peritoneal cavity were isolated and analyzed using RNA sequencing.

The RNA-seq data obtained from murine peritoneal macrophages reveal a very small variance between the WT and embigin knockout mice, indicating that not many genes are differentially expressed in the peritoneal macrophages of mice when embigin is knocked out (Figure 15). However, one interesting protein was identified in the results. *Smoc1* is upregulated by about 162% in the embgin KO samples compared to the WT (Figure 15).

A)

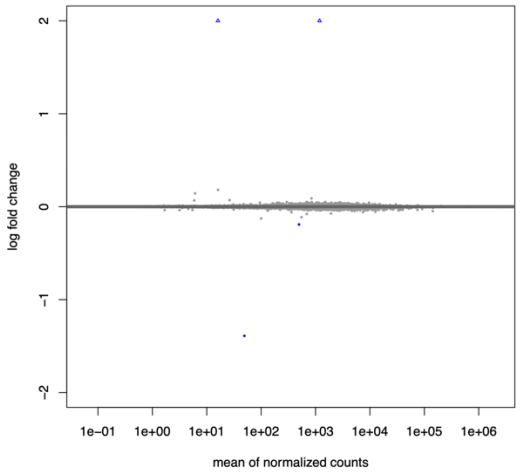

B)

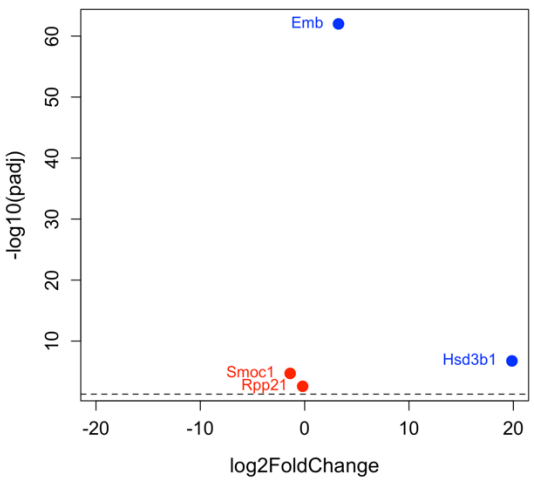

C)

Symbol	Protein	log2FoldChange	FoldChange (higher in WT)	padj
EMB	Embigin	3.24	9.47	1.00E-62
Smoc1	SPARC related modular calcium binding 1	-1.39	-2.62	2.80E-02
Rpp21	ribonuclease P 21 subunit	-0.19	-1.14	1.00E-54

D)

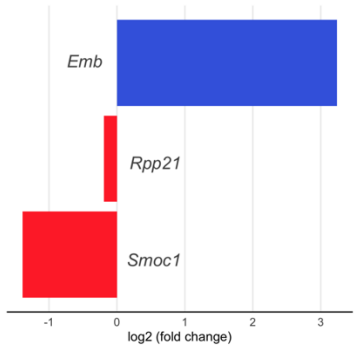

Figure 15. WT and Emb$^{-/-}$ mice do not show much variation between them; however, *Smoc1* is differentially expressed with an upregulation in the Emb$^{-/-}$ mice. A) Sample variance of murine peritoneal macrophages with the WT and the EMB-KO phenotype. Very few genes are being differentially expressed across the two phenotypes. **B)** Volcano plot for mouse peritoneal macrophages. The blue genes (*Emb* and *Hsd3b1*) are upregulated in the WT samples, while the red genes (*Smoc1* and *Rpp21*) are downregulated in WT mice when compared to the Emb$^{-/-}$ samples. **C)** Table of differentially expressed

genes in the peritoneal macrophages of mice samples. Negative values show a downregulation in the WT compared with Emb$^{-/-}$ mice. **D)** Differential expression bar plot for mouse peritoneal macrophages. Embigin in blue represents the WT sample, while the genes in red demonstrate a downregulation in WT compared to the Emb$^{-/-}$ samples.

Beyond the transcription level, embigin is subsequently translated into several glycosylated states of embigin in the murine peritoneal macrophages and is present at the protein level (Figure 16).

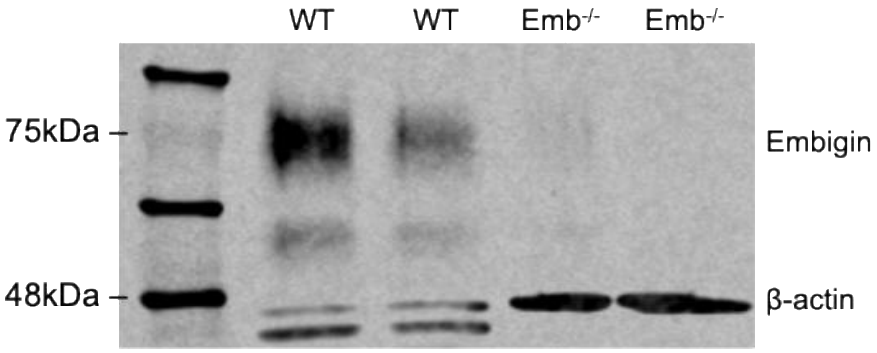

Figure 16. Embigin is translated into a smear of glycosylated states of proteins in the mouse peritoneal macrophages. The Emb$^{-/-}$ samples do not express any embigin protein. SDS-PAGE with an 8% gel was used to run the samples for western blotting.

4.8 Detection of SMOC1 in murine peritoneal macrophages at the protein level

With the RNA sequencing results of the mouse peritoneal macrophage samples suggesting SMOC1 as a new study target candidate, being upregulated in the Emb$^{-/-}$ mice, Western blot experiments were performed to analyze SMOC1 protein expression in the murine peritoneal macrophages; however, SMOC1 is a secreted protein, and these protein samples were acquired from the lysed mouse macrophages and not the original culture media.

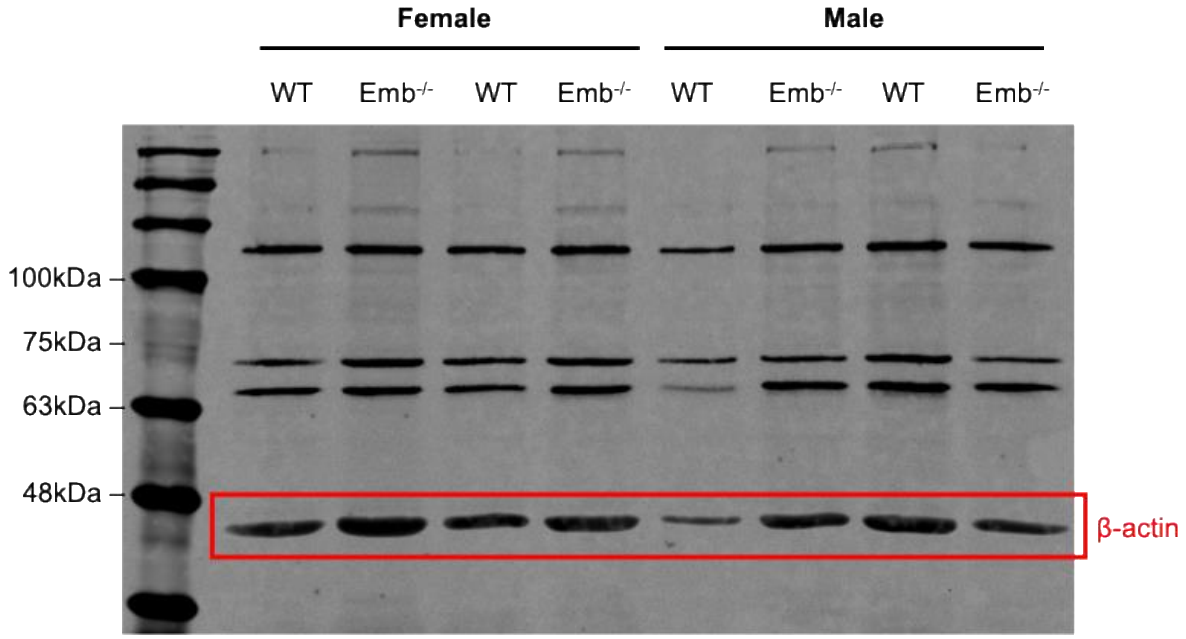

Figure 17. The detection of SMOC1 proteins in mouse peritoneal samples was inconclusive. The expected band size for SMOC1 is between 50 and 60 kDa. SDS-PAGE with an 8% gel was used to run the samples for western blotting.

Based on the manufacturer's instructions for the anti-mouse-SMOC-1 antibody (ab313571), the expected observable band would fall between 50 and 60 kDa; however, no distinct band was observed in the specified range. In addition, multiple non-specific bands were visible, which deemed the results of this experiment inconclusive (Figure 17).

4.9 Visualization of embigin and MCTs localized in murine peritoneal macrophages

As established by previous studies, embigin acts as an ancillary protein for MCT1, facilitating its localization into the plasma membrane (Xu et al., 2022). With the aim of determining if embigin has a similar function in association with MCT1 in macrophages *in vivo*, immunofluorescence staining experiments were designed to visualize both embigin and MCT1 in peritoneal macrophages acquired from an 8-week-old WT mouse. The cells were stained for embigin (in red), MCT1 (in green), and the nucleus using DAPI (in blue). The results from the samples were inconsistent; only a fraction of the cells were positive for embigin (Figure 18).

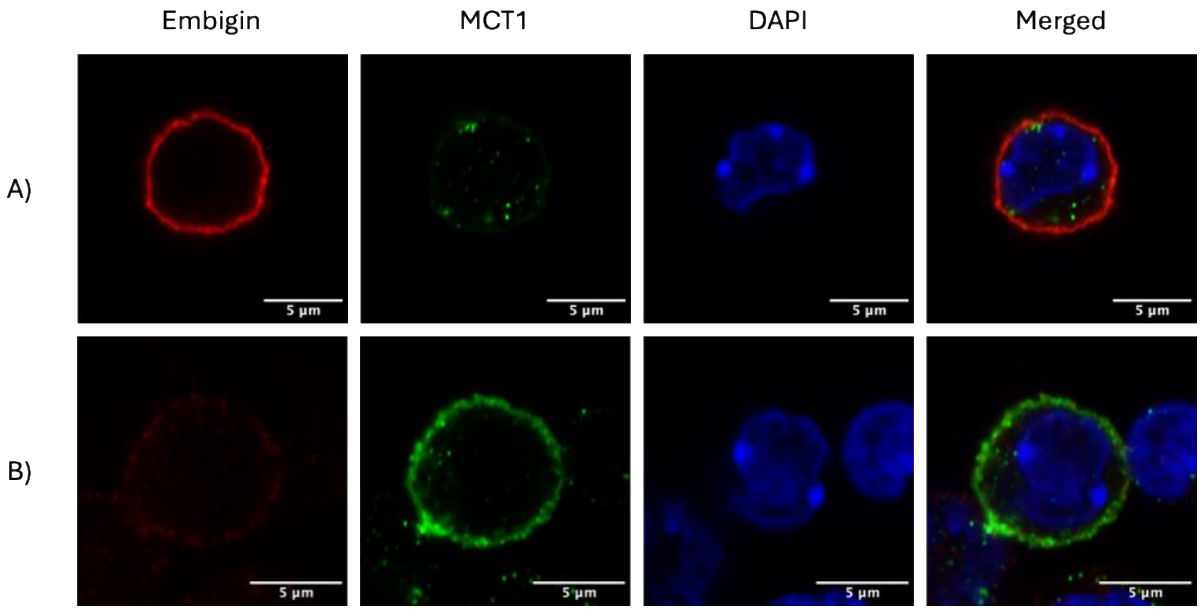

Figure 18. Immunofluorescent staining of mouse peritoneal macrophages demonstrated an inconsistent pattern in cells being positive for embigin and MCT1. The cells are stained for embigin in red, MCT1 in green, and the nuclei of the cells are stained with DAPI. **A)** Some cells demonstrate high levels of embigin with low levels of MCT1, while **B)** others display high levels of MCT1 with low levels of embigin.

With further analysis, it was noticed that some of the cells in the sample displayed a high expression of embigin but a low expression of MCT1 (Figure 18, A), whereas in other cells of the same sample, the reverse was observed (Figure 18, B). This inconsistency makes these results unreliable.

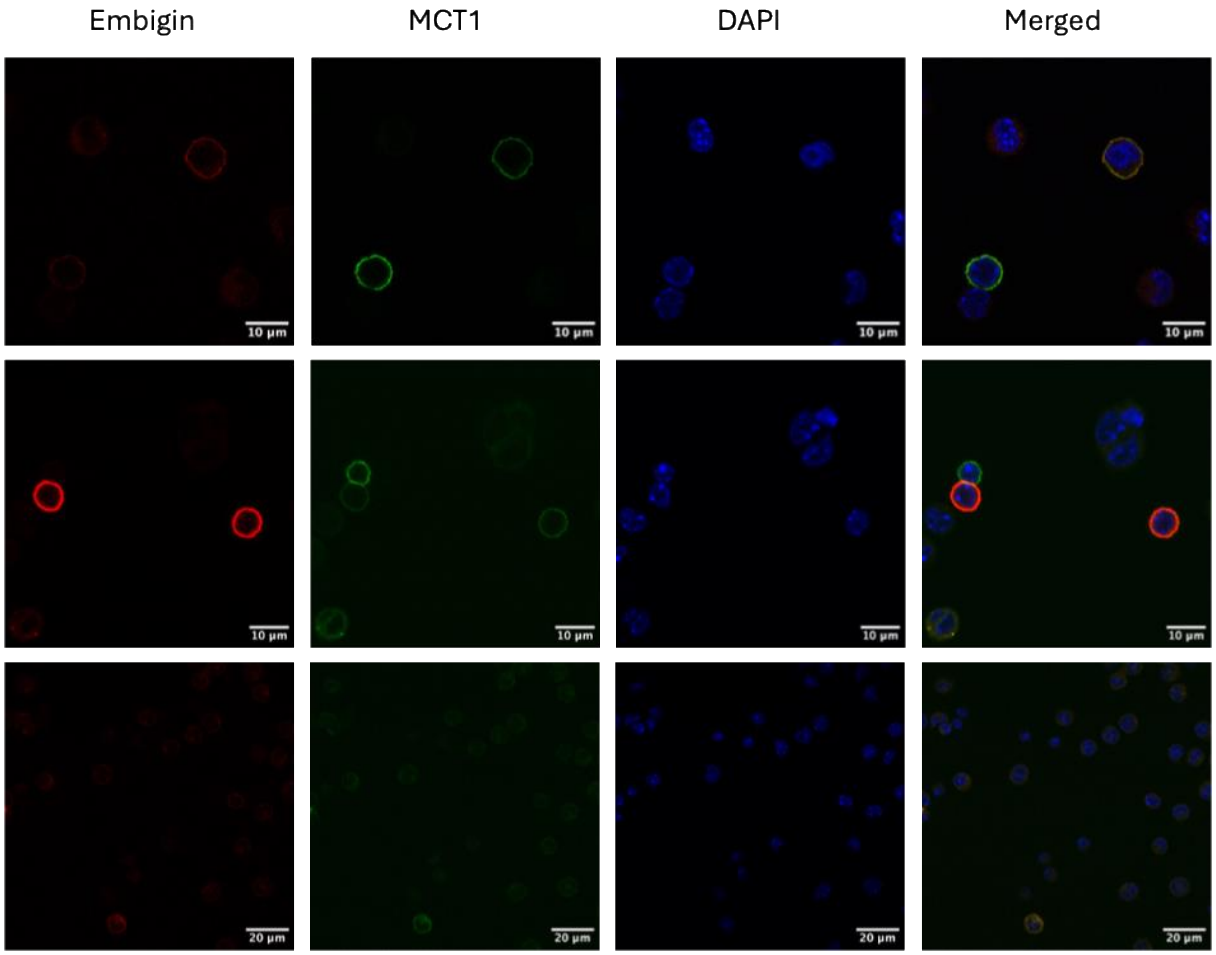

Figure 19. The control immunofluorescence experiment shows a very high inconsistency in the specific binding of the secondary antibody to the primary antibody in the samples. Immunofluorescent staining of mouse peritoneal macrophages was performed only with secondary antibodies as a negative control. Some cells display high green signals, some high in red, and some cells are very faint and only display DAPI, which is expected for negative controls.

To address the observed inconsistencies in the samples, a negative control sample was prepared, incubated only in exposure to the secondary antibodies, to ensure that the primary antibodies were specifically binding to embigin and MCT1. These control samples were also very inconsistent. In some cells, only the nuclei were stained, which was expected; however, other patterns of non-specific primary antibody bindings were also observed (Figure 19). These inconclusive results highlighted potential other factors in play that prevent the specific bindings.

4.10 Sex-related variations in the murine peritoneal macrophage population

When analysing the RNA concentrations of the peritoneal macrophages acquired from mouse samples, interesting variations by sex were observed in the similarly aged 8–12-week-old mice. In this sample set, the RNA concentration can be considered as a measure of the number of macrophages localized in the peritoneal cavity of male and female mice.

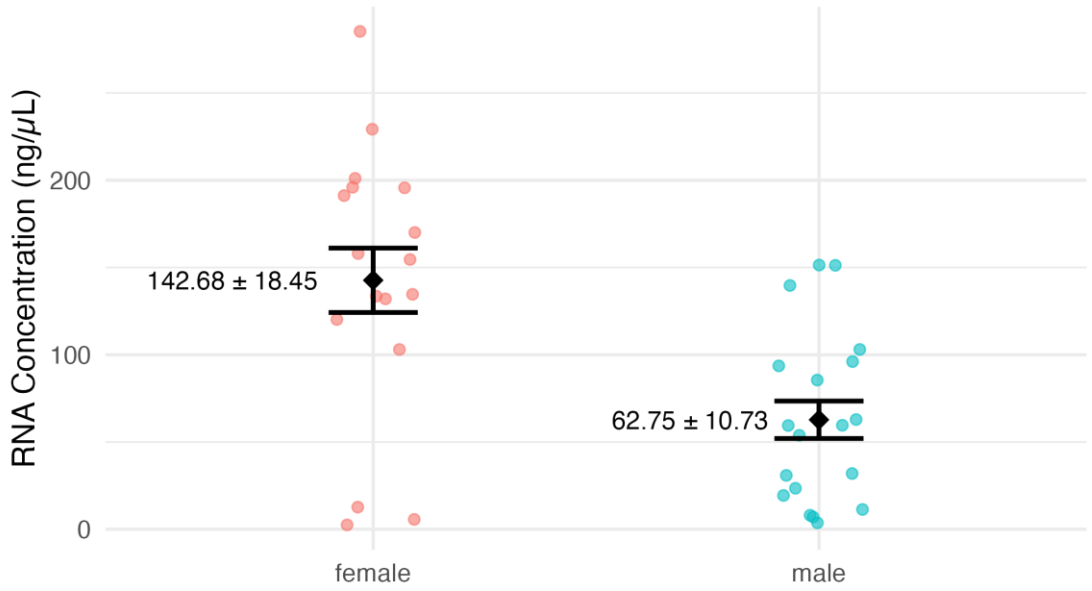

Figure 20. Female mice exhibit more than twice the number of macrophages localized in the peritoneal cavity compared to male samples. Scatter plot of RNA concentration of the isolated peritoneal macrophages from 8–12-week-old mice. The concentration can be considered as a measure of macrophage population size. The plot displays the mean ± SD. Welch's two-sample t-test p-value: 0.001.

According to the results, females have more than twice (2.27 ratio) the amount of RNA (p-value: 0.001), which reflects a higher number of macrophages localized in the peritoneal cavity of female mice compared to males (Figure 20).

To avoid any variations between the genotypes, WT and Emb$^{-/-}$, a multivariable comparison was also performed, and the results were consistent, showing minimal variation between genotypes (Figure 21), suggesting that sex may be a factor in determining the number of localized macrophages in the peritoneal cavity of 8- to 12-week-old mice.

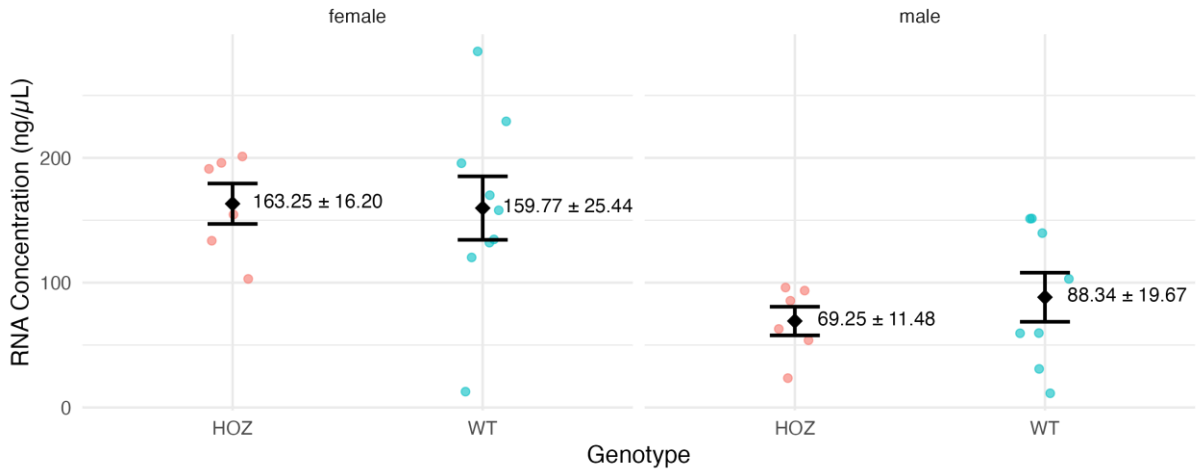

Figure 21. Genotype has very minimal variation in the number of macrophages localized in the peritoneal cavity of mice, while sex plays a significant role. RNA concentration of the isolated peritoneal macrophages from 8–12-week-old mice. The concentration can be considered as a measure of macrophage population size. The plot displays the mean ± SD. HOZ: Emb$^{-/-}$ mice.

Overall, after several experiments performed on samples acquired from human and murine origins, this study finds that embigin is differentially expressed in macrophage populations, with an upregulation of 47% in the M2-like compared to M1-like macrophages. Additionally, the embigin protein is found to be expressed at higher levels in the M2a macrophage subtypes compared with M2, M2c, and M2d subtypes. Furthermore, MCTs are differentially expressed between the pro- and anti-inflammatory macrophages, with MCT1, MCT6, and MCT8 being upregulated in human M2-like macrophages while MCT2, MCT4, and MCT10 are downregulated in comparison to M1-like macrophages. Although these transcriptomic results obtained with bulk RNA sequencing are significant, at the single-cell resolution, macrophages display high levels of diversity, where not all macrophage clusters express embigin at a high level, along with the observed differentially expressed pattern of the MCTs, which underlines how single-cell methods are crucial in understanding biological systems.

Although the RNA sequencing results from the mouse peritoneal samples did not demonstrate much variance between the WT and Emb$^{-/-}$, the data suggest SMOC1 as a new study candidate, which is differentially expressed between the two genotypes. This study confirmed that embigin is expressed in the WT mice at the protein level, and attempted to detect SMOC1 as well, which was not conclusive. Moreover,

immunofluorescence staining experiments were performed to attempt to visualize and validate associations between embigin and MCT1 in murine peritoneal macrophages; however, valid results were not acquired. Additionally, lactate assays were carried out to measure lactate transport between the macrophages and the extracellular space, but the results were not statistically significant. Finally, this study found a sex-related difference in the number of localized macrophages in the peritoneal cavity of mice. Female mice exhibit more than double the number of localized peritoneal macrophages when compared to male mice, which highlights another degree of complexity in macrophage regulation and immune responses between the two sexes.

5 Discussion

This study aimed to investigate the expression profile and the potential functional roles of the surface glycoprotein, embigin, in different macrophage population samples with both mouse and human origins. Embigin is a member of the basigin family proteins, along with basigin and neuroplastin, all of which share similar structural and functional properties. Embigin has been shown to act as an ancillary protein for certain MCTs, facilitating their transport to the plasma membrane (Xu et al., 2022). In addition, studies have demonstrated that embigin can also function as an ECM receptor by direct binding to fibronectin (Sipilä et al., 2022). Recent studies have shown that embigin also plays a regulatory role in the development of lungs in mice (Talvi et al., 2024). These findings highlight a potential for embigin in linking cellular metabolism, lactate transport, cell adhesion, and embryonic development. Despite the research efforts to study embigin, its expression and potential functions in macrophages remain understudied.

5.1 Embigin expression and relevance in macrophages

The findings of this study indicate that embigin is upregulated in the anti-inflammatory M2-like macrophages compared to the pro-inflammatory M1-like cells. The evidence suggests that embigin transcript levels are heightened in human M2-like macrophage spheroids by a fold change of 1.47, along with a unique differential expression profile for MCTs. We found that in M2-like macrophages, MCT1 is upregulated with a fold change of 2.30, while MCT4 and MCT2 are downregulated with fold changes of -2.45 and -1.88, respectively. Although MCT1-4 are known to be bidirectional transporters, MCT4 is known to be mainly a lactate exporter, while MCT1 and MCT2 are recognized as lactate importers, with MCT2 being a high-affinity lactate importer, which functions mainly under low lactate concentrations; on the other hand, MCT1 has a lower affinity to lactate and has been shown to become functional when intercellular lactate levels are elevated (Maculewicz et al., 2025). The results from this study align with these previously established concepts, where MCT1 is upregulated, and MCT2 is downregulated, noting a heightened extracellular lactate concentration, and MCT4 is downregulated to minimize

lactate export and maximize the uptake instead. Furthermore, the lactate assay results, although not statistically significant, demonstrate an increase in the cell culture lactate concentration in the embigin knockdown samples, which indicates that when embigin levels are low, the metabolic regulation changes in favor of lactate export, which is consistent with the transcript level results. This suggests a potential link between the expression of embigin and the regulation of lactate uptake in anti-inflammatory macrophages under high lactate concentrations.

In addition, we found that at the protein level, embigin is being expressed at the highest level in the M2a macrophages, followed by M2c and M2d macrophages. The M2a macrophages were polarized using IL-4 and IL-13, the M2c were polarized by IL-10 incubation, and the M2d by IL-6. One possible explanation for this finding may be that embigin expression is correlated with the extent of the macrophage anti-inflammatory activity. The anti-inflammatory extent of M2a, M2c, and M2d is consistent with the theoretical framework proposed by Murray et al. (2014), where macrophages polarized by IL-4 are introduced as the anti-inflammatory extreme of the macrophage polarization spectrum, and cells polarized by IL-10 are not as extreme in their anti-inflammatory phenotype (Murray et al., 2014). This pattern may reflect a link between higher embigin expression and higher anti-inflammatory activity.

5.2 SMOC1 is differentially expressed between WT and Emb$^{-/-}$ mice

Previous studies have characterized murine peritoneal macrophages (PM) as mainly anti-inflammatory M2-like macrophages under homeostatic conditions (Ardavín et al., 2023). When PMs taken from mouse samples were analyzed by RNA sequencing, SMOC1, a protein shown to have a possible functional role in regulating macrophage phagocytic activity, emerged as a differentially expressed factor between the WT and Emb$^{-/-}$ mice, being upregulated in the Emb$^{-/-}$ mice. This might imply that higher embigin levels correlate with a downregulation in SMOC1.

Previous research has shown M2-like macrophages to have a higher rate and capacity for phagocytosis, since these macrophages are tasked with clearing large amounts of

apoptotic cells and debris (Suleimanov et al., 2024). Other findings previously studied by Ukan et al. (2022) revealed that higher SMOC1 levels are linked to heightened macrophage phagocytosis (Ukan et al., 2022). We find embigin to be upregulated in the M2-like anti-inflammatory macrophages and SMOC1 to be downregulated, which introduces a new level of complexity to this matter. Firstly, not all macrophages localized in the peritoneal cavity of mice can be considered as M2-like, secondly, phagocytosis is a complex process with several regulatory factors, and finally, the phagocytic activity of anti-inflammatory macrophages is dependent on the specific M2 subtype, which cannot be determined when analyzing a large and diverse population such as the peritoneal macrophages; these arguments can explain why a decrease in SMOC1 transcripts in bulk RNA sequencing is not sufficient evidence to conclude that SMOC1 is downregulated in the M2-like macrophages. These questions remain highly valuable since PM polarization and activity are especially relevant in tumor contexts.

5.3 Sex-related differences in murine PM population sizes

Additionally, this study found that the RNA concentration of female murine PMs is nearly double that of the male mice. Since the PM isolation protocol includes a cell adhesion-based step for purifying macrophages and removing the other cell types present in the peritoneal cavity, the RNA concentration can be considered as a measure of the total macrophage population size in mice. The data suggest that these variations are sex-dependent and do not relate to the genotype of the mice. This finding consistently aligns with previous research indicating that female mice and rats have a higher number of localized leukocytes, including B and T lymphocytes and macrophages, in the peritoneal cavity compared to the male animals (Scotland et al., 2011). These insights underline a new level of complexity for future immunology research since the sex difference is very high and may result in different physiological outcomes.

5.4 Study limitations

Several limitations of this study should be acknowledged. Firstly, the lactate assay runs resulted in a high sample variation, which could be mitigated by a higher number of replicates; in addition, further optimization of the protocol may result in clearer data points. The immunofluorescence staining results were highly inconsistent, although the study attempted to control for non-specific primary antibody binding. The observed results are most probably due to the secondary antibodies binding to the highly variable Fc receptors on the surface of the macrophages (Pyzik et al., 2023).

Furthermore, there are limitations and complexities involved when conducting research with multiple organism samples. Although both humans and mice are mammals and highly similar in terms of physiological and cellular properties, there are species-specific variations between them that need to be noted. Sex-related variations also exist, as this study finds a different number of macrophages in female and male mice, which highlights that further research needs to account for sex-related differences as well.

Another limitation arises in studying SMOC1, especially in Western blots. Since SMOC1 is a glycoprotein secreted to the extracellular space (Wang et al., 2022), it was challenging to perform Western blots for SMOC1 after the protein samples were acquired from the mice without knowing that the culture media may contain SMOC1. Another simple limitation was the time constraints, since this research is a master's thesis project and not a very comprehensive research effort that can re-run experiments entirely to account for the limitations of the protocols.

5.5 Future directions and conclusion

Future studies are required to further understand the functional roles of embigin in macrophages. This study has provided new potential targets that can be studied more extensively, for instance, SMOC1, which has been known to be associated with phagocytic activity, and here is shown to be upregulated with the knockout of embigin. Since this study discovered SMOC1 in bulk RNA sequencing of mouse PMs, a new possible future direction would be to analyze SMOC1 in human-derived samples to

identify the extent of expression and potential functions of SMOC1 in human-derived macrophages. Moreover, with the complexity and heterogeneity of macrophage populations, single-cell methods, such as single-cell RNA sequencing, can be employed in future studies to characterize human samples and investigate SMOC1 and embigin associations, among other potential study targets. Since SMOC1 is a secreted glycoprotein, new experiments could also be designed to optimize SMOC1 isolation and quantification.

SMOC1-related proteins are also appropriate candidates for a subsequent study combining SMOC1 functions with embigin presence (Figure 23). Additionally, future efforts can focus on the lactate and the general metabolic landscape of macrophages and how it links to embigin levels.

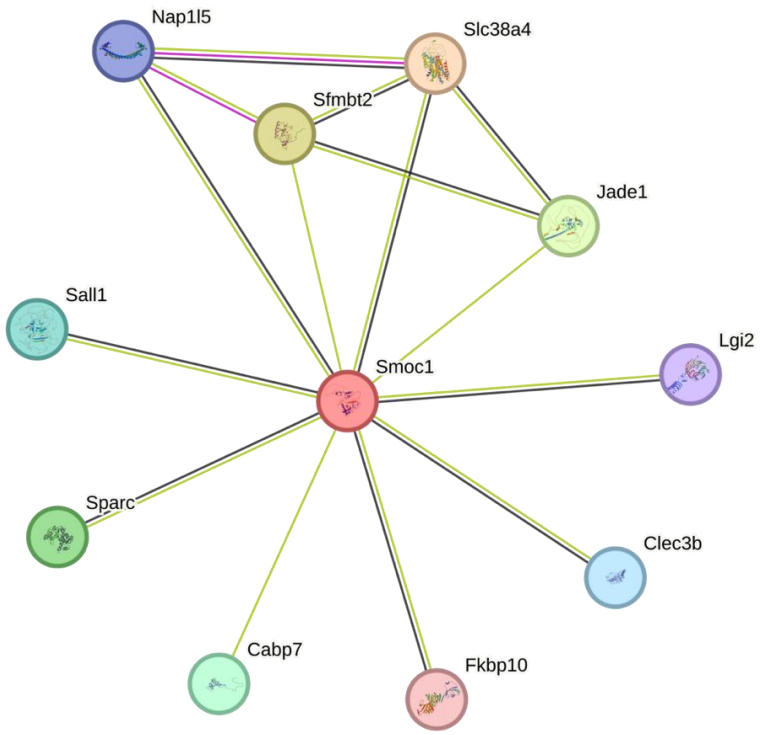

Figure 22. A predicted network of functional partners of Smoc1, a regulator of osteoblast differentiation involved in eye and limb development, is also known to associate with phagocytic activity. Each node represents all proteins encoded by a single protein-coding gene locus, with splice isoforms and post-translational modifications collapsed. Smoc1 is shown as the central node (red). Surrounding first-shell interactors are also shown as colored nodes, each with filled icons indicating a known or predicted 3D protein structure. Edges represent predicted functional associations, proteins that jointly contribute to a shared function, rather than direct physical binding. All edges in this network are derived from text mining (yellow-green lines) and protein homology (light purple lines), with no experimentally determined or curated database interactions detected among these partners. Network was generated using STRING v12.0.

In conclusion, this study provides evidence that embigin is being differentially expressed between macrophage subtype populations, with M2-like anti-inflammatory macrophages demonstrating an increase in embigin expression compared to the M1-like pro-inflammatory macrophages. Additionally, the embigin protein is being expressed at the highest levels in M2a macrophage subtypes, which are extremely anti-inflammatory. In addition, we find embigin to have associations with MCT-mediated lactate transport, with an overall regulation of MCT members to maximize cellular lactate uptake. Tumors are known to have extracellular lactate buildup, which can be an energy source for either the oxidative tumor cells or the anti-inflammatory supportive TAMs. Embigin expression may have a facilitative role in the regulation of lactate transport and TAM polarization. Finally, we suggest SMOC1 as a candidate for future studies, linking inflammatory activity and phagocytic activity.

Together, these findings have several theoretical and practical implications in cancer immunology research. With future research on embigin, it, or its related partner proteins and pathways, could be considered as possible therapeutic targets.

References

Afonso, J., Santos, L. L., Miranda-Gonçalves, V., Morais, A., Amaro, T., Longatto-Filho, A., & Baltazar, F. (2015). CD147 and MCT1-potential partners in bladder cancer aggressiveness and cisplatin resistance. *Molecular Carcinogenesis*, *54*(11), 1451–1466. https://doi.org/10.1002/mc.22222

Anders, S., Pyl, P. T., & Huber, W. (2015). HTSeq—A Python framework to work with high-throughput sequencing data. *Bioinformatics*, *31*(2), 166–169. https://doi.org/10.1093/bioinformatics/btu638

Ardavín, C., Alvarez-Ladrón, N., Ferriz, M., Gutiérrez-González, A., & Vega-Pérez, A. (2023). Mouse Tissue-Resident Peritoneal Macrophages in Homeostasis, Repair, Infection, and Tumor Metastasis. *Advanced Science*, *10*(11), 2206617. https://doi.org/10.1002/advs.202206617

Beesley, P., Kraus, M., & Parolaro, N. (2014). The Neuroplastins: Multifunctional Neuronal Adhesion Molecules—Involvement in Behaviour and Disease. In V. Berezin & P. S. Walmod (Eds.), *Cell Adhesion Molecules* (Vol. 8, pp. 61–89). Springer New York. https://doi.org/10.1007/978-1-4614-8090-7_4

Cassado, A. D. A., Dâ€™ImpÃ©rio Lima, M. R., & Bortoluci, K. R. (2015). Revisiting Mouse Peritoneal Macrophages: Heterogeneity, Development, and Function. *Frontiers in Immunology*, *6*. https://doi.org/10.3389/fimmu.2015.00225

Chen, L., Lin, Y., Zhu, X., Zhuo, S., Li, Z., Guo, C., Ye, X., Chen, J., Wang, S., & Chen, Y. (2025). MCT1-mediated Lactate Shuttle to Mitochondria Governs Macrophage Polarization and Modulates Glucose Homeostasis by Affecting β Cells. *Advanced Science*, *12*(38), e14760. https://doi.org/10.1002/advs.202414760

Chen, S., Saeed, A. F. U. H., Liu, Q., Jiang, Q., Xu, H., Xiao, G. G., Rao, L., & Duo, Y. (2023). Macrophages in immunoregulation and therapeutics. *Signal Transduction and Targeted Therapy*, *8*(1), 207. https://doi.org/10.1038/s41392-023-01452-1

Cheng, B., Liu, J., Gao, L., Zhu, Z., Yang, Y., Liu, S., & Wu, X. (2025). EMB-driven glioblastoma multiforme progression via the MCT4/GPX3 axis: Therapeutic inhibition by Ganxintriol A. *Journal of Translational Medicine*, *23*(1), 272. https://doi.org/10.1186/s12967-025-06290-z

De Jesus, A., Pusec, C. M., Nguyen, T., Keyhani-Nejad, F., Gao, P., Weinberg, S. E., & Ardehali, H. (2022). Optimized protocol to isolate primary mouse peritoneal macrophage metabolites. *STAR Protocols*, *3*(4), 101668. https://doi.org/10.1016/j.xpro.2022.101668

Dobin, A., Davis, C. A., Schlesinger, F., Drenkow, J., Zaleski, C., Jha, S., Batut, P., Chaisson, M., & Gingeras, T. R. (2013). STAR: Ultrafast universal RNA-seq aligner. *Bioinformatics*, *29*(1), 15–21. https://doi.org/10.1093/bioinformatics/bts635

Ewels, P., Magnusson, M., Lundin, S., & Käller, M. (2016). MultiQC: Summarize analysis results for multiple tools and samples in a single report. *Bioinformatics*, *32*(19), 3047–3048. https://doi.org/10.1093/bioinformatics/btw354

Felmlee, M. A., Jones, R. S., Rodriguez-Cruz, V., Follman, K. E., & Morris, M. E. (2020). Monocarboxylate Transporters (SLC16): Function, Regulation, and Role in Health and Disease. *Pharmacological Reviews*, *72*(2), 466–485. https://doi.org/10.1124/pr.119.018762

Geistlinger, K., Schmidt, J. D. R., & Beitz, E. (2023). Human monocarboxylate transporters accept and relay protons via the bound substrate for selectivity and activity at physiological pH. *PNAS Nexus*, *2*(2), pgad007. https://doi.org/10.1093/pnasnexus/pgad007

Goswami, K. K., Bose, A., & Baral, R. (2021). Macrophages in tumor: An inflammatory perspective. *Clinical Immunology*, *232*, 108875. https://doi.org/10.1016/j.clim.2021.108875

Guan, F., Wang, R., Yi, Z., Luo, P., Liu, W., Xie, Y., Liu, Z., Xia, Z., Zhang, H., & Cheng, Q. (2025). Tissue macrophages: Origin, heterogenity, biological functions, diseases and therapeutic targets. *Signal Transduction and Targeted Therapy*, *10*(1), 93. https://doi.org/10.1038/s41392-025-02124-y

Guenette, R. S., Sridhar, S., Herley, M., Mooibroek, M., Wong, P., & Tenniswood, M. (1997). Embigin, a developmentally expressed member of the immunoglobulin super family, is also expressed during regression of prostate and mammary gland. *Developmental Genetics*, *21*(4), 268–278. https://doi.org/10.1002/(SICI)1520-6408(1997)21:4%253C268::AID-DVG4%253E3.0.CO;2-5

Guillaume, J., Leufgen, A., Hager, F. T., Pabst, O., & Cerovic, V. (2023). MHCII expression on gut macrophages supports T cell homeostasis and is regulated by microbiota

and ontogeny. *Scientific Reports*, *13*(1), 1509. https://doi.org/10.1038/s41598-023-28554-8

Hao, Y., Stuart, T., Kowalski, M. H., Choudhary, S., Hoffman, P., Hartman, A., Srivastava, A., Molla, G., Madad, S., Fernandez-Granda, C., & Satija, R. (2024). Dictionary learning for integrative, multimodal and scalable single-cell analysis. *Nature Biotechnology*, *42*(2), 293–304. https://doi.org/10.1038/s41587-023-01767-y

Higuchi, K., Sugiyama, K., Tomabechi, R., Kishimoto, H., & Inoue, K. (2022). Mammalian monocarboxylate transporter 7 (MCT7/Slc16a6) is a novel facilitative taurine transporter. *Journal of Biological Chemistry*, *298*(4), 101800. https://doi.org/10.1016/j.jbc.2022.101800

Huang, R.-P., Ozawa, M., Kadomatsu, K., & Muramatsu, T. (1993). Embigin, a Member of the Immunoglobulin Superfamily Expressed in Embryonic Cells, Enhances Cell-Substratum Adhesion. *Developmental Biology*, *155*(2), 307–314. https://doi.org/10.1006/dbio.1993.1030

Jin, X., Zhang, N., Yan, T., Wei, J., Hao, L., Sun, C., Zhao, H., & Jiang, S. (2025). Lactate-mediated metabolic reprogramming of tumor-associated macrophages: Implications for tumor progression and therapeutic potential. *Frontiers in Immunology*, *16*, 1573039. https://doi.org/10.3389/fimmu.2025.1573039

Kallio, M. A., Tuimala, J. T., Hupponen, T., Klemelä, P., Gentile, M., Scheinin, I., Koski, M., Käki, J., & Korpelainen, E. I. (2011). Chipster: User-friendly analysis software for microarray and other high-throughput data. *BMC Genomics*, *12*(1), 507. https://doi.org/10.1186/1471-2164-12-507

Koltai, T., & Fliegel, L. (2024). Exploring monocarboxylate transporter inhibition for cancer treatment. *Exploration of Targeted Anti-Tumor Therapy*, *5*(1), 135–169. https://doi.org/10.37349/etat.2024.00210

Li, M., Yang, Y., Xiong, L., Jiang, P., Wang, J., & Li, C. (2023). Metabolism, metabolites, and macrophages in cancer. *Journal of Hematology & Oncology*, *16*(1), 80. https://doi.org/10.1186/s13045-023-01478-6

Love, M. I., Huber, W., & Anders, S. (2014). Moderated estimation of fold change and dispersion for RNA-seq data with DESeq2. *Genome Biology*, *15*(12), 550. https://doi.org/10.1186/s13059-014-0550-8

Ma, R.-Y., Black, A., & Qian, B.-Z. (2022). Macrophage diversity in cancer revisited in the era of single-cell omics. *Trends in Immunology*, *43*(7), 546–563. https://doi.org/10.1016/j.it.2022.04.008

Maculewicz, E., Bojarczuk, A., Mastalerz, A., Johne, M., Mróz, A., Garbacz, A., & Stastny, P. (2025). Associations Between Genetic Variants in MCT2 (rs3763980, rs995343, rs3763979) and MCT4 (rs11323780) with Blood Lactate Kinetics Before and After Supramaximal Exercise. *International Journal of Molecular Sciences*, *26*(16), 7865. https://doi.org/10.3390/ijms26167865

Martinez, F. O., & Gordon, S. (2014). The M1 and M2 paradigm of macrophage activation: Time for reassessment. *F1000Prime Reports*, *6*. https://doi.org/10.12703/P6-13

Miyauchi, T., Masuzawa, Y., & Muramatsu, T. (1991). The Basigin Group of the Immunoglobulin Superfamily: Complete Conservation of a Segment in and around Transmembrane Domains of Human and Mouse Basigin and Chicken HT7 Antigen. *The Journal of Biochemistry*, *110*(5), 770–774. https://doi.org/10.1093/oxfordjournals.jbchem.a123657

Mosser, D. M., & Edwards, J. P. (2008). Exploring the full spectrum of macrophage activation. *Nature Reviews Immunology*, *8*(12), 958–969. https://doi.org/10.1038/nri2448

Murray, P. J., Allen, J. E., Biswas, S. K., Fisher, E. A., Gilroy, D. W., Goerdt, S., Gordon, S., Hamilton, J. A., Ivashkiv, L. B., Lawrence, T., Locati, M., Mantovani, A., Martinez, F. O., Mege, J.-L., Mosser, D. M., Natoli, G., Saeij, J. P., Schultze, J. L., Shirey, K. A., … Wynn, T. A. (2014). Macrophage Activation and Polarization: Nomenclature and Experimental Guidelines. *Immunity*, *41*(1), 14–20. https://doi.org/10.1016/j.immuni.2014.06.008

Okada, I., Hamanoue, H., Terada, K., Tohma, T., Megarbane, A., Chouery, E., Abou-Ghoch, J., Jalkh, N., Cogulu, O., Ozkinay, F., Horie, K., Takeda, J., Furuichi, T., Ikegawa, S., Nishiyama, K., Miyatake, S., Nishimura, A., Mizuguchi, T., Niikawa, N., … Saitsu, H. (2011). SMOC1 Is Essential for Ocular and Limb Development in Humans and Mice. *The American Journal of Human Genetics*, *88*(1), 30–41. https://doi.org/10.1016/j.ajhg.2010.11.012

O'Neill, L. A. J., Kishton, R. J., & Rathmell, J. (2016). A guide to immunometabolism for immunologists. *Nature Reviews Immunology*, *16*(9), 553–565. https://doi.org/10.1038/nri.2016.70

Ozawa, M., Huang, R. P., Furukawa, T., & Muramatsu, T. (1988). A teratocarcinoma glycoprotein carrying a developmentally regulated carbohydrate marker is a member of the immunoglobulin gene superfamily. *Journal of Biological Chemistry*, *263*(7), 3059–3062. https://doi.org/10.1016/S0021-9258(18)69032-5

Pavlides, S., Whitaker-Menezes, D., Castello-Cros, R., Flomenberg, N., Witkiewicz, A. K., Frank, P. G., Casimiro, M. C., Wang, C., Fortina, P., Addya, S., Pestell, R. G., Martinez-Outschoorn, U. E., Sotgia, F., & Lisanti, M. P. (2009). The reverse Warburg effect: Aerobic glycolysis in cancer associated fibroblasts and the tumor stroma. *Cell Cycle*, *8*(23), 3984–4001. https://doi.org/10.4161/cc.8.23.10238

Payen, V. L., Mina, E., Van Hée, V. F., Porporato, P. E., & Sonveaux, P. (2020). Monocarboxylate transporters in cancer. *Molecular Metabolism*, *33*, 48–66. https://doi.org/10.1016/j.molmet.2019.07.006

Pyzik, M., Kozicky, L. K., Gandhi, A. K., & Blumberg, R. S. (2023). The therapeutic age of the neonatal Fc receptor. *Nature Reviews Immunology*, *23*(7), 415–432. https://doi.org/10.1038/s41577-022-00821-1

Qian, Y., Galan-Cobo, A., Guijarro, I., Dang, M., Molkentine, D., Poteete, A., Zhang, F., Wang, Q., Wang, J., Parra, E., Panda, A., Fang, J., Skoulidis, F., Wistuba, I. I., Verma, S., Merghoub, T., Wolchok, J. D., Wong, K.-K., DeBerardinis, R. J., … Heymach, J. V. (2023). MCT4-dependent lactate secretion suppresses antitumor immunity in LKB1-deficient lung adenocarcinoma. *Cancer Cell*, *41*(7), 1363-1380.e7. https://doi.org/10.1016/j.ccell.2023.05.015

Rainger, J., Van Beusekom, E., Ramsay, J. K., McKie, L., Al-Gazali, L., Pallotta, R., Saponari, A., Branney, P., Fisher, M., Morrison, H., Bicknell, L., Gautier, P., Perry, P., Sokhi, K., Sexton, D., Bardakjian, T. M., Schneider, A. S., Elcioglu, N., Ozkinay, F., … FitzPatrick, D. R. (2011). Loss of the BMP Antagonist, SMOC-1, Causes Ophthalmo-Acromelic (Waardenburg Anophthalmia) Syndrome in Humans and Mice. *PLoS Genetics*, *7*(7), e1002114. https://doi.org/10.1371/journal.pgen.1002114

Ross, E. A., Devitt, A., & Johnson, J. R. (2021). Macrophages: The Good, the Bad, and the Gluttony. *Frontiers in Immunology*, *12*, 708186. https://doi.org/10.3389/fimmu.2021.708186

Schindelin, J., Arganda-Carreras, I., Frise, E., Kaynig, V., Longair, M., Pietzsch, T., Preibisch, S., Rueden, C., Saalfeld, S., Schmid, B., Tinevez, J.-Y., White, D. J., Hartenstein, V., Eliceiri, K., Tomancak, P., & Cardona, A. (2012). Fiji: An open-source platform for biological-image analysis. *Nature Methods*, *9*(7), 676–682. https://doi.org/10.1038/nmeth.2019

Schmidt, N., Kollewe, A., Constantin, C. E., Henrich, S., Ritzau-Jost, A., Bildl, W., Saalbach, A., Hallermann, S., Kulik, A., Fakler, B., & Schulte, U. (2017). Neuroplastin and Basigin Are Essential Auxiliary Subunits of Plasma Membrane Ca2+-ATPases and Key Regulators of Ca2+ Clearance. *Neuron*, *96*(4), 827-838.e9. https://doi.org/10.1016/j.neuron.2017.09.038

Scotland, R. S., Stables, M. J., Madalli, S., Watson, P., & Gilroy, D. W. (2011). Sex differences in resident immune cell phenotype underlie more efficient acute inflammatory responses in female mice. *Blood*, *118*(22), 5918–5927. https://doi.org/10.1182/blood-2011-03-340281

Silberstein, L., Goncalves, K. A., Kharchenko, P. V., Turcotte, R., Kfoury, Y., Mercier, F., Baryawno, N., Severe, N., Bachand, J., Spencer, J. A., Papazian, A., Lee, D., Chitteti, B. R., Srour, E. F., Hoggatt, J., Tate, T., Lo Celso, C., Ono, N., Nutt, S., … Scadden, D. T. (2016). Proximity-Based Differential Single-Cell Analysis of the Niche to Identify Stem/Progenitor Cell Regulators. *Cell Stem Cell*, *19*(4), 530–543. https://doi.org/10.1016/j.stem.2016.07.004

Silva, A., Cerqueira, M. C., Rosa, B., Sobral, C., Pinto-Ribeiro, F., Costa, M. F., Baltazar, F., & Afonso, J. (2023). Prognostic Value of Monocarboxylate Transporter 1 Overexpression in Cancer: A Systematic Review. *International Journal of Molecular Sciences*, *24*(6), 5141. https://doi.org/10.3390/ijms24065141

Sipilä, K., Rognoni, E., Jokinen, J., Tewary, M., Vietri Rudan, M., Talvi, S., Jokinen, V., Dahlström, K. M., Liakath-Ali, K., Mobasseri, A., Du-Harpur, X., Käpylä, J., Nutt, S. L., Salminen, T. A., Heino, J., & Watt, F. M. (2022). Embigin is a fibronectin receptor that affects sebaceous gland differentiation and metabolism. *Developmental Cell*, *57*(12), 1453-1465.e7. https://doi.org/10.1016/j.devcel.2022.05.011

Strizova, Z., Benesova, I., Bartolini, R., Novysedlak, R., Cecrdlova, E., Foley, L. K., & Striz, I. (2023). M1/M2 macrophages and their overlaps – myth or reality? *Clinical Science*, *137*(15), 1067–1093. https://doi.org/10.1042/CS20220531

Suleimanov, S. K., Efremov, Y. M., Klyucherev, T. O., Salimov, E. L., Ragimov, A. A., Timashev, P. S., & Vlasova, I. I. (2024). Radical-Generating Activity, Phagocytosis, and Mechanical Properties of Four Phenotypes of Human Macrophages. *International Journal of Molecular Sciences*, *25*(3), 1860. https://doi.org/10.3390/ijms25031860

Suwal, U. (2025). *Matrisome and Tumor Microenvironment in Cancer Progression*. University of Turku.

Takahata, Y., Hagino, H., Kimura, A., Urushizaki, M., Kobayashi, S., Wakamori, K., Fujiwara, C., Nakamura, E., Yu, K., Kiyonari, H., Bando, K., Murakami, T., Komori, T., Hata, K., & Nishimura, R. (2021). Smoc1 and Smoc2 regulate bone formation as downstream molecules of Runx2. *Communications Biology*, *4*(1), 1199. https://doi.org/10.1038/s42003-021-02717-7

Talvi, S., Jokinen, J., Rappu, P., Leppäkoski, R., Kurtzeborn, K., Rantakari, P., Kuure, S., & Heino, J. (2026). Embigin is involved in the regulation of early mouse kidney development. *Scientific Reports*, *16*(1), 8403. https://doi.org/10.1038/s41598-026-39966-7

Talvi, S., Jokinen, J., Sipilä, K., Rappu, P., Zhang, F.-P., Poutanen, M., Rantakari, P., & Heino, J. (2024). Embigin deficiency leads to delayed embryonic lung development and high neonatal mortality in mice. *iScience*, *27*(2), 108914. https://doi.org/10.1016/j.isci.2024.108914

Tao, H., Zhong, X., Zeng, A., & Song, L. (2023). Unveiling the veil of lactate in tumor-associated macrophages: A successful strategy for immunometabolic therapy. *Frontiers in Immunology*, *14*, 1208870. https://doi.org/10.3389/fimmu.2023.1208870

Ukan, Ü., Delgado Lagos, F., Kempf, S., Günther, S., Siragusa, M., Fisslthaler, B., & Fleming, I. (2022). Effect of Thrombin on the Metabolism and Function of Murine Macrophages. *Cells*, *11*(10), 1718. https://doi.org/10.3390/cells11101718

Wang, Y., Gu, J., Du, A., Zhang, S., Deng, M., Zhao, R., Lu, Y., Ji, Y., Shao, Y., Sun, W., & Kong, X. (2022). SPARC-related modular calcium binding 1 regulates aortic valve

calcification by disrupting BMPR-II/p-p38 signalling. *Cardiovascular Research*, *118*(3), 913–928. https://doi.org/10.1093/cvr/cvab107

Wilson, M. C., Meredith, D., Fox, J. E. M., Manoharan, C., Davies, A. J., & Halestrap, A. P. (2005). Basigin (CD147) Is the Target for Organomercurial Inhibition of Monocarboxylate Transporter Isoforms 1 and 4. *Journal of Biological Chemistry*, *280*(29), 27213–27221. https://doi.org/10.1074/jbc.M411950200

Xu, B., Zhang, M., Zhang, B., Chi, W., Ma, X., Zhang, W., Dong, M., Sheng, L., Zhang, Y., Jiao, W., Shan, Y., Chang, W., Wang, P., Wen, S., Pei, D., Chen, L., Zhang, X., Yan, H., & Ye, S. (2022). Embigin facilitates monocarboxylate transporter 1 localization to the plasma membrane and transition to a decoupling state. *Cell Reports*, *40*(11), 111343. https://doi.org/10.1016/j.celrep.2022.111343

Xu, B., Zhou, X., Shan, Y., Shi, S., Li, J., Liang, Q., Wang, Z., Zhang, M., Wang, Y., Pei, D., & Ye, S. (2025). Structure-guided screening identifies Tucatinib as dual inhibitor for MCT1/2. *EMBO Reports*, *27*(3), 677–703. https://doi.org/10.1038/s44319-025-00661-9

Zhang, Q., & Sioud, M. (2023). Tumor-Associated Macrophage Subsets: Shaping Polarization and Targeting. *International Journal of Molecular Sciences*, *24*(8), 7493. https://doi.org/10.3390/ijms24087493

Zhang, Y., Jiang, H., Dong, M., Min, J., He, X., Tan, Y., Liu, F., Chen, M., Chen, X., Yin, Q., Zheng, L., Shao, Y., Li, X., & Chen, H. (2024). Macrophage MCT4 inhibition activates reparative genes and protects from atherosclerosis by histone H3 lysine 18 lactylation. *Cell Reports*, *43*(5), 114180. https://doi.org/10.1016/j.celrep.2024.114180

Acknowledgments

This master's thesis project was carried out in the Interaction of Cells with the Extracellular Matrix group at the Department of Life Technologies at the Faculty of Technology, University of Turku. The experiments and laboratory work were performed in the facilities provided by the MediCity Research Laboratory, the Central Animal Laboratory of the University of Turku (UTUCAL), and the Cell Imaging and Cytometry Core (CIC) of the Turku Bioscience Center, all located at BioCity, Turku.

I would like to thank my supervisors, Dr. Johanna Jokinen and Docent Elina Siljamäki, for this great opportunity and their guidance. I have learned many things throughout my work for this master's thesis, and I am truly grateful. I would like to extend my gratitude to our principal investigator, Prof. Jyrki Heino, for his leadership and knowledge, which have been a great inspiration that has fueled my curiosity to pursue immunology.

I appreciate all the kind support and knowledge of the other Heino group members: Docent Pekka Rappu, Emmi Virtanen, Liisa Pösö, Dr. Ujjwal Suwal, Docent Jarmo Käpylä, Maria Tuominen, and a special thanks to Dr. Salli Talvi for her invaluable guidance and assistance in conducting animal experiments. I would also like to acknowledge the mice whose sacrifices made this study possible.

I am very grateful to my mother, Prof. Afsaneh Zonouzi, for her unconditional support and advice, who always praises me to pursue my passions. I would like to thank my brothers, Dr. Alireza Rahmani and Mohammad Rahmani, as well, for their support throughout my journey. I sincerely extend my gratitude to all my friends who accompanied me through all my personal and academic challenges. Finally, I dedicate this thesis to my father, Prof. Hossein Rahmani, who always believed in me and encouraged me that every question worth asking is worth chasing.

Sajad Rahmani

June 2026

Use of Artificial Intelligence

This study was assisted by the limited use of artificial intelligence. ChatGPT (OpenAI) and Claude (Anthropic) were the main tools used for summarizing research articles and searching for relevant studies in the field, as well as debugging R scripts and providing assistance in some calculations. Perplexity (Perplexity AI, Inc.) was used as a search engine and assistant in quick queries on different basic biological concepts to save time while researching. In the process of writing the thesis, Grammarly (Superhuman Platform Inc.) was utilized to correct inaccurate grammatical structures.